AD-A038 916 NORTH CAROLINA UNIV AT CHAPEL HILL DEPT OF CHEMISTRY F/6 7/4
A STUDY OF THE ELECTRICAL PROPERTIES OF THE CHARGE-TRANSFER DER--ETC(U)
APR 77 C W ANDREWS, J R WASSON, W E HATFIELD N00014-76-C-0816

UNCLASSIFIED TR-2 NL

| OF |
AD
A038916

END

DATE
FILMED
5-77

12

FC

OFFICE OF NAVAL RESEARCH

Contract N00014-76-C-0816

Task No. NR 053-617

TECHNICAL REPORT NO. 2

A Study of the Electrical Properties of the Charge-Transfer Derivatives of Diaminoanthraquinones

by

C. Webster Andrews III, John R. Wasson, and William E. Hatfield

University of North Carolina
Department of Chemistry
Chapel Hill, North Carolina 27514

April 1, 1977

SECURITY CLASSIFICATION OF THIS PAGE (When Data Entered)

REPORT DOCUMENTATION PAGE

READ INSTRUCTIONS BEFORE COMPLETING FORM

1. REPORT NUMBER: Technical Report No. 2
2. GOVT ACCESSION NO.:
3. RECIPIENT'S CATALOG NUMBER:
4. TITLE (and Subtitle): A Study of the Electrical Properties of the Charge-Transfer Derivatives of Diaminoanthraquinones.
5. TYPE OF REPORT & PERIOD COVERED: Interim rept.
6. PERFORMING ORG. REPORT NUMBER:
7. AUTHOR(s): C. Webster Andrews, III, John R. Wasson and William E. Hatfield
8. CONTRACT OR GRANT NUMBER(s): N00014-76-C-0816
9. PERFORMING ORGANIZATION NAME AND ADDRESS: The University of North Carolina, Department of Chemistry, Chapel Hill, North Carolina 27514
10. PROGRAM ELEMENT, PROJECT, TASK AREA & WORK UNIT NUMBERS: NR 053-617
11. CONTROLLING OFFICE NAME AND ADDRESS: Office of Naval Research, Department of the Navy, Arlington, Virginia 22217
12. REPORT DATE: 1 April 1977
13. NUMBER OF PAGES: 58
14. MONITORING AGENCY NAME & ADDRESS (if different from Controlling Office):
15. SECURITY CLASS. (of this report): Unclassified
15a. DECLASSIFICATION/DOWNGRADING SCHEDULE:
15. DISTRIBUTION STATEMENT (of this Report): Approved for Public Release, Distribution Unlimited
17. DISTRIBUTION STATEMENT (of the abstract entered in Block 20, if different from Report):
18. SUPPLEMENTARY NOTES:
19. KEY WORDS (Continue on reverse side if necessary and identify by block number):
Cyclic voltametry
Electron paramagnetic resonance
Diaminoanthraquinones
Copper Complexes
Charge-Transfer Compounds
Semi conductors
20. ABSTRACT (Continue on reverse side if necessary and identify by block number):
Charge-transfer complexes of 1,2-diaminoanthraquinone, 1,4-diaminoanthraquinone, 1,5-diaminoanthraquinone and phenothiazine with copper(II) halides and/or iodine have been prepared and characterized by physiochemical techniques including cyclic voltametry and resistivity measurements. The conducting properties of the compounds were found to be related to the electrochemical behavior.

DD FORM 1 JAN 73 1473 EDITION OF 1 NOV 65 IS OBSOLETE

Unclassified

SECURITY CLASSIFICATION OF THIS PAGE (When Data Entered)

A Study of the Electrical Properties of the Charge-Transfer Derivatives of Diaminoanthraquinones

C. Webster Andrews III, John R. Wasson and William E. Hatfield

Department of Chemistry
Venable Hall and Kenan Laboratories 045A
University of North Carolina
Chapel Hill, North Carolina 27514

TABLE OF CONTENTS

Introduction

The charge-transfer reaction

$$D: + A \longrightarrow (D^{\cdot+})(A^{\cdot-})$$

has been successfully used to synthesize highly conducting molecular complexes from non-conducting constituent molecules. In electronic terms, the process involves the transfer of an electron from the highest filled orbital of the donor D to the lowest unfilled orbital of the acceptor A. During recent years, considerable research has been undertaken to evaluate the molecular parameters responsible for high conductivity in these charge-transfer salts. Several excellent reviews on the subject are available,[1] but a brief synopsis is given here as background.

Organic charge-transfer reactions produce radical cations and/or radical anions. These radicals must be stable to decomposition and coupling reactions since the existence of unpaired electrons is a necessary condition for conductivity.[2] The unpaired electrons are believed to be the charge carriers.[3] For charge transfer to occur under moderate conditions, the donor must have a low ionization potential and the acceptor should have a high electron affinity.[4] It is essential that planar molecules be used since molecular stacking in the solid state is a prerequisite for band formation. The now classic examples of highly conducting molecular solids, i.e. the charge-transfer derivatives of the planar organic molecule tetracyanoquinodimethane (TCNQ)[5] and the square-planar coordination complex $K_2Pt(CN)_4$, contain one-dimensional columns of planar molecules stacked face-to-face.[6] It is apparent that the free electrons and holes created by charge-transfer are delocalized along these columns. There are other crucial requirements, e.g. the stacking must be segregated, uniform, and closely spaced, which must be met before delocalization is realized, but which are difficult to control synthetically.[7]

The above guidelines are consistent with the available experimental evidence, but in general it is difficult to design new conducting systems. Ionization potentials and electron affinities for organic molecules are not widely known and crystal structures cannot be predicted a priori. In practice, the best method of approach often proves to be trial and error. Conductivity measurements on chemical systems are not trivial, but can be performed rapidly and accurately with the proper equipment thereby allowing the screening of a large number of potentially conducting compounds. This is essential if information is to be gained by variation of chemical parameters.

One of the goals of this project was the design of a conductivity cell that would allow rapid and accurate measurement of conductivity. Having accomplished this, the next goal was to find a new chemical system(s) with high conductivity. The final goal was to characterize the electrical properties of that system(s) using variable-frequency and variable-temperature conductivity measurements, cyclic voltammetry, electron-spin resonance, and absorption spectroscopy.

It was discovered that the addition products of a series of diaminoanthraquinones with molecular iodine and copper(II) halides showed radically different electrical properties. The structure of 1,2-diaminoanthraquinone (1,2-DAAQ), 1,4-diaminoanthraquinone(1,4-DAAQ), and 1,5-diaminoanthraquinone (1,5-DAAQ) are presented in Figure 1. The results of the investigations spawned by this series of molecules is reported herein. In addition, the charge-transfer salt of phenothiazine (PH) and iodine was reinvestigated. This was deemed important because there are inconsistencies in the literature concerning the electrical properties of this salt.[8]

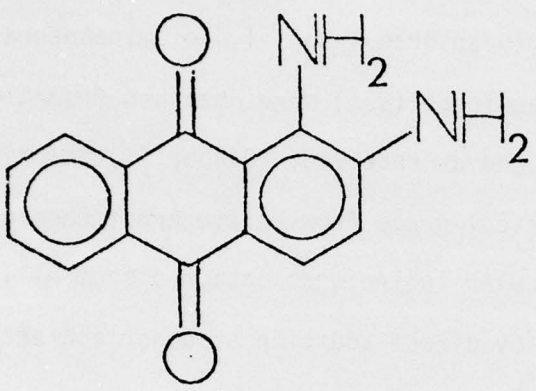

1,2-DAAQ

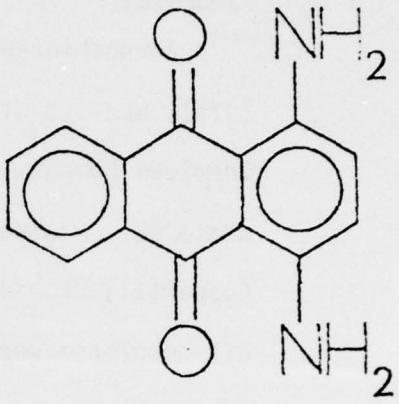

1,4-DAAQ

FIGURE 1. Molecular Structures

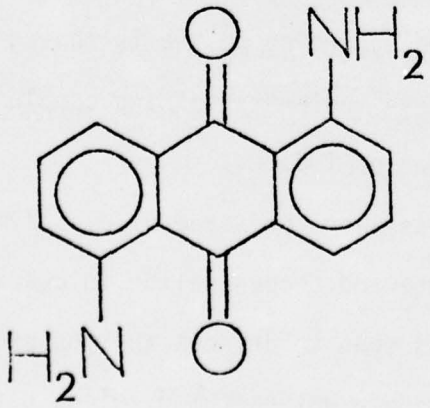

1,5-DAAQ

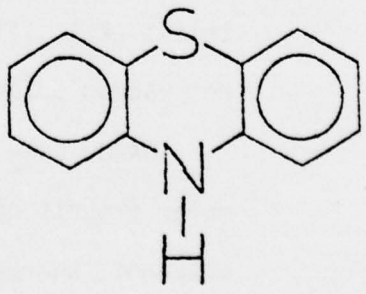

PHENOTHIAZINE

Synthesis

Phenothiazine, 1,2-diaminoanthraquinone, 1,4-diaminoanthraquinone (97%), and 1,5-diaminoanthraquinone (97%) were obtained from Aldrich Chemical Company, and were used as received. Copper(II) chloride dihydrate was obtained in analytical grade from Mallinckrodt Chemical Works. Copper(II) bromide and molecular iodine were obtained from Allied Chemical. All complexes were prepared by direct addition of donor and acceptor.

DAAQ·I_2 complexes were prepared by dispersing and mixing stoichiometric amounts of diaminoanthraquinone with iodine in a small volume of carbon tetrachloride, whereupon the mixture was taken to dryness and ground to a fine powder. This sequence was repeated several times until a homogeneous product was obtained. No washing or filtration was used to isolate the product; hence, the product stoichiometry is the reactant stoichiometry. Once it was established (see below) that complexes containing 1,4-DAAQ were highly conducting, it became of interest to determine what ratio of 1,4-DAAQ to iodine would generate the lowest resistivity. Complexes were therefore synthesized according to the following stoichiometries: 2:1, 1:1, 2:3, and 1:2. These iodine-containing complexes were not vacuum dried to avoid sublimation of iodine.

DAAQ · CuX_2 (X = Cl, Br) complexes were prepared by dissolving equimolar amounts of diaminoanthraquinone and copper halide in absolute methanol, whereupon the solution was spun to dryness and the product ground to a fine powder. This procedure was executed twice, but on the third cycle, the wet product was isolated by suction filtration and dried

overnight under vacuum.

The PH·I_2 complex was prepared by dissolving phenothiazine and iodine in a 2:3 molar ratio in acetonitrile and spinning the solution to dryness, whereupon the product was isolated without washing or filtration.

The various reactant stoichiometries are reported along with the product stoichiometries, with analyses where available, in Table 1. Three 1,4-DAAQ adducts and the phenothiazine complex were analyzed by Galbraith Laboratories of Knoxville, Tennessee and the analyses are reported in Table 2. The large deviations from the theoretical stoichiometries seen for some elements indicate the non-stoichiometry of these charge-transfer complexes. It should be noticed that the analytic stoichiometry for 1,4-DAAQ·$CuBr_2$ is 3:2. This differs from the analytical stoichiometry observed for 1,4-DAAQ·$CuCl_2$ which is 1:1. The difference probably lies in the larger size of bromide versus chloride anion.

The Resistivity Measurement

1. Preparation of Samples by Compaction

Single crystals of the materials under study were not available, so samples of each were prepared as compactions. The products were first vacuum dried, where possible, to remove all traces of solvent and moisture (water, methanol, and acetonitrile are conducting media) whereupon they were thoroughly ground into fine powders for uniformity. The powders were then compacted into rigid pellets, 1.30 cm in diameter by 0.2 cm thick, using a Beckman KBr die and 25 ton Ring Press. In order that each sample could be meaningfully compared, ten tons of pressure was used to compact each pellet.

TABLE 1

Synthesis of Charge-Transfer Complexes

Donor + Acceptor	Reactant Stoichiometry	Product Stoichiometry*
Phenothiazine + I_2	2:3	2:3
1,4-DAAQ + I_2	2:1	
	1:1	
	2:3	2:3
	1:2	
1,4-DAAQ + $CuCl_2$	1:1	1:1
1,4-DAAQ + $CuBr_2$	1:1	3:2
1,2-DAAQ + $CuCl_2$	1:1	
1,2-DAAQ + $CuBr_2$	1:1	
1,5-DAAQ + I_2	2:3	
1,5-DAAQ + $CuCl_2$	1:1	

*When available.

TABLE 2

Analysis of Selected Charge-Transfer Complexes

Complex	Element	% Theoretical	% Observed
phenothiazine·I_2(2:3)	C	24.85	24.97
	H	1.56	1.57
	N	2.42	2.38
1,4-DAAQ·I_2(2:3)	C	27.17	28.84
	H	1.63	1.75
	N	4.53	4.53
1,4-DAAQ·$CuCl_2$(1:1)	C	45.12	45.46
	H	2.71	3.25
	N	7.52	6.80
1,4-DAAQ·$CuBr_2$(3:2)	C	43.43	43.52
	H	2.60	2.81
	N	7.40	6.90

Measurements taken on single crystals are enormously more reliable for the following reasons: a) The resistivity of a compacted sample is a function of the applied pressure, and it is always greater than the single crystal value. This is due to interparticle contact resistance, which arises at the grain boundaries during compaction. b) The presence of this resistance serves to distort the activation energy.[9] c) Single crystals are usually anisotropic in resistivity, but this information is lost using compressed powders since each grain is randomly oriented in the pellet. Measurements on compacted samples are therefore strictly semi-quantitative. They are suitable for characterization, however, especially when single crystals are not available. Evidence[10] suggests that the resistivity of a compacted sample averages no more than two orders of magnitude above single crystal values, and it must be borne in mind that the resistivity spectrum spans almost thirty orders of magnitude.

2. Resistivity (and Conductivity) from Resistance.

Resistivity, ρ, has units of ohm-centimeters and is directly related to the resistance of the sample by a geometric factor as follows:

$$\rho = R \frac{(\text{area})}{(\text{length})} .$$

For cylindrical pellets, the length is just the thickness. In practice the resistance is usually calculated from Ohm's Law by measuring the voltage drop induced by passing a known, constant current between two opposite faces of the sample ($R = \frac{V}{I}$). Conductivity, σ, is just the reciprocal of resistivity and has units of reciprocal ohm-centimeters.

3. The Resistance Measurement

The conductivity cell used to obtain resistance measurements in this project is shown in Figure 2. The sample, a, is held between two flat,

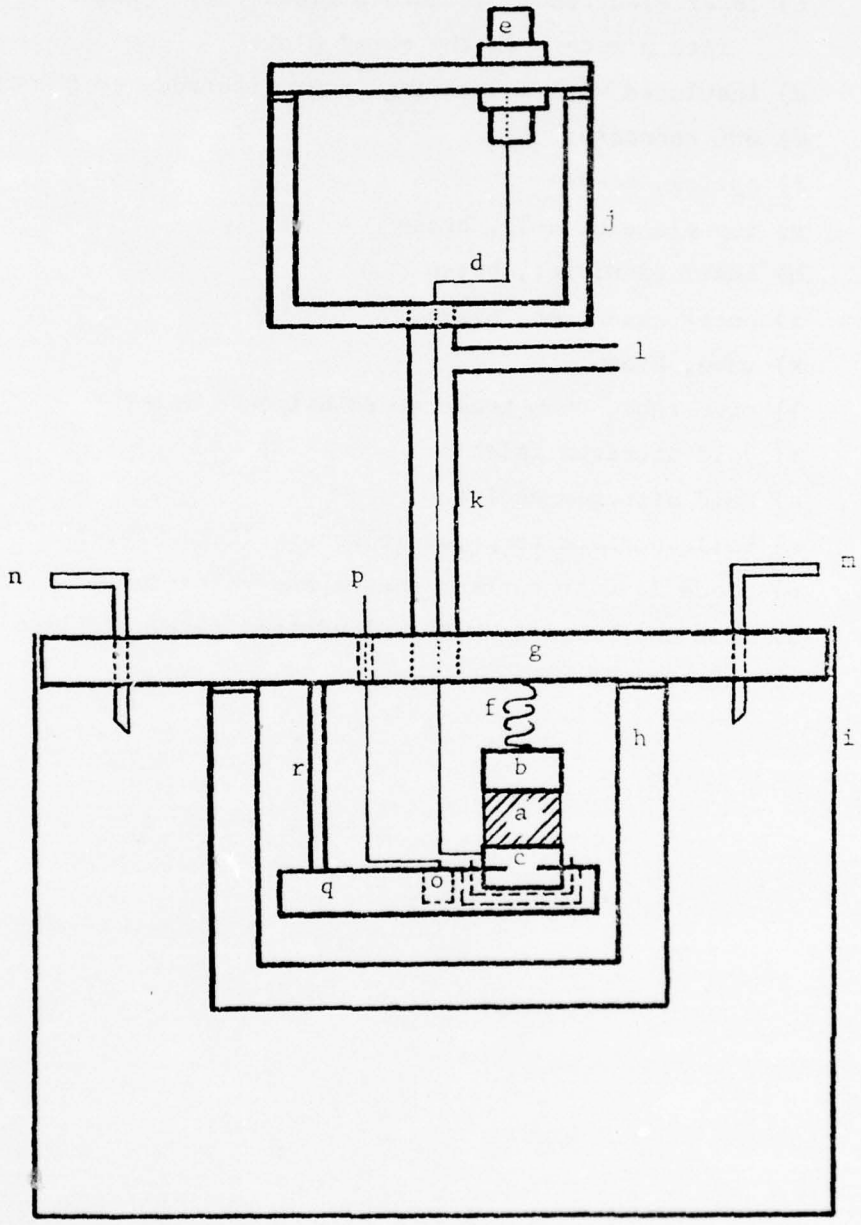

FIGURE 2. The Conductivity Cell

KEY TO FIGURE 2:

a) sample
b) upper electrode
c) lower electrode, fit into a glass cup, which fits into a recess in the metal plate
d) insulated wire connecting lower electrode to BNC connector
e) BNC connector
f) spring, steel
g) top plate of cell, brass
h) inner cannister, brass
i) outer cannister, brass
k) tube, brass
l) side tube, room temperature nitrogen inlet
m) cold nitrogen inlet
n) cold nitrogen outlet
o) silicon diode temperature sensor (Lake Shore)
p) diode lead to current source and voltmeter
q) 1/4" copper plate with cylindrical recess drilled 3/16" deep
r) support rod

spring-loaded copper electrodes, b and c. The upper electrode connects to the outer terminal of a BNC connector e through the case and is at ground potential. The lower electrode is insulated from the case and connects to the inner BNC terminal. This circuitry was adapted from an apparatus designed by Mr. R.J. Lieb[11] of the UNC-CH Department of Physics. The resistance measurement consists of connecting the electrode assembly to a Kiethley 227 Current Source (d.c.) via the BNC connector, applying a current, and reading the induced voltage drop from a voltmeter connected across the current leads.

The advantages of using this particular two-probe conductivity cell are that it allows rapid interchanging of samples and facile calibration using standard resistors. The cell is designed so that the electrodes can be easily removed from the apparatus for cleanings, which is a requirement for each new sample. With prolonged use, an oxide surface layer forms, and this can be easily removed by acid treatment or grinding. In addition, the actual hardware used in this project included three cells so that three samples could be measured simultaneously during a low temperature run. The extra cells were accomodated by drilling two additional recessions in the small metal plate, g, shown in Figure 2. Each cell was connected to its own BNC connector. The advantages achieved by reducing experimental time and nitrogen consumption were enormous.

The one disadvantage associated with two-probe measurements is the possibility of contact resistance, which sometimes arises at the electrode-sample interfaces and causes the measured resistance of the sample to be abnormally high. This resistance is non-ohmic however, and can be detected

by measuring the resistance of the sample at several small d.c. currents. If the resistance does not vary, then it may be assumed that contact resistance is absent.[12] The standard way to circumvent this problem is to utilize a four-probe electrode arrangement.

All samples used in this project were tested in the cell for contact resistance. Only the $CuCl_2$ adduct of 1,4-DAAQ showed recurring contact resistance and it should be realized that the resistivity reported for this compound is probably greater than the value intrinsic to the sample.

4. Cryogenic Equipment

Variable temperature resistance measurements are essential in the electrical characterization of a solid. The low temperature instrumentation and technique reported here were adapted from that described by J.G. Fitz.[13]

The conductivity cell described above is equipped with two brass cannisters for cryogenic temperature control (see Figure 2). The electrode assembly is bolted inside the smaller cannister, h which, in turn, is bolted inside the larger container, i. Nitrogen gas from a pressurized tank is passed through a coil of copper tubing immersed in a dewar containing liquid nitrogen. The chilled gas exits the coil and enters the space between the outer and inner cannisters via the inlet m, thus cooling the sample. The temperature of the gas is controlled by varying the flow rate through the coil. The inner cannister is purged with a small flow of room temperature nitrogen to prevent freezing of moisture on the electrode assembly and sample. The whole apparatus is fit inside a large styrofoam block lined with aluminum foil and covered with glass wool for thermal insulation. The sample temperature can be taken to 77°K by using a high flow rate and adequate insulation.

The temperature is monitored with a calibrated silicon diode, o, obtained from Lake Shore Cryotronics, Inc.,[14] that was mounted in the center of the copper plate, q, holding the electrode assembly. The diode is driven with a constant current of ten microamperes, which induces a temperature-dependent voltage drop measured by voltmeter. A least squares plot of the linear portion of the calibration table provided by Lake Shore resulted in an equation for the temperature as a function of diode voltage and this equation was used to calculate the sample temperature. The use of a diode rather than the traditional thermocouple results in a greatly simplified temperature measurement and allows direct observation of the rate of temperature change.

Resistance versus Frequency Measurements

Compaction of powdered materials gives rise to interparticle contact resistance, with the result that the observed resistance is the sum of the single crystal value plus the interparticle contribution. Huggins and Sharbaugh[15] have proposed an attractive method for eliminating this interparticle component. Their theory and method are reviewed and expanded here, with a discussion of instrumentation.

The two sources of resistance in a compacted sample, namely, the material itself and the grain boundaries, are also sources of capacitance. To a first approximation, the resistance and capacitance of each source are connected in parallel, and both parallel RC combinations are connected in series, as shown in the equivalent circuit in Figure 3a. R_s and C_s are the sample resistance and capacitance, respectively, and R_{ipc} and C_{ipc}

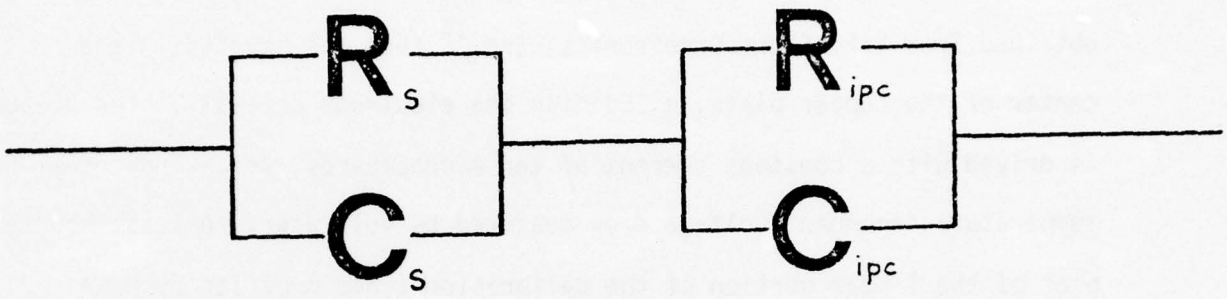

FIGURE 3a. Equivalent Circuit for Compacted Samples

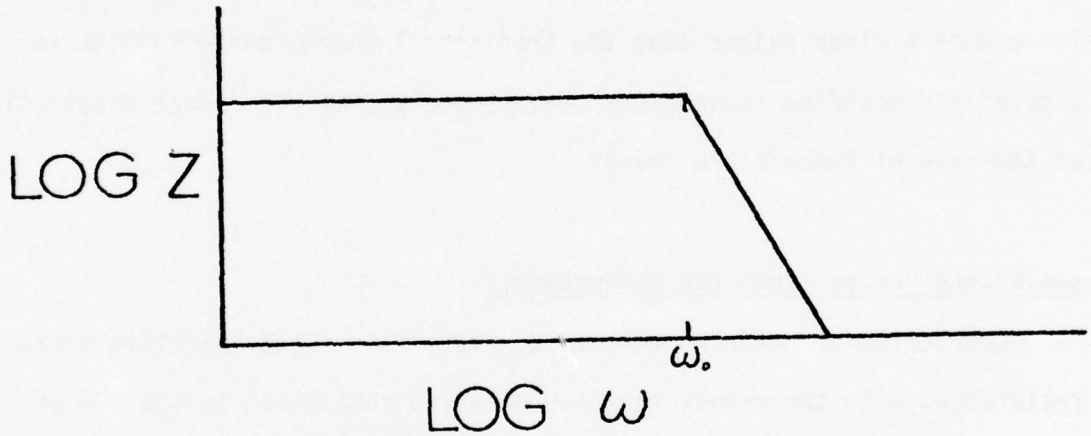

FIGURE 3b. Idealized Bode Plot for One Parallel RC Circuit

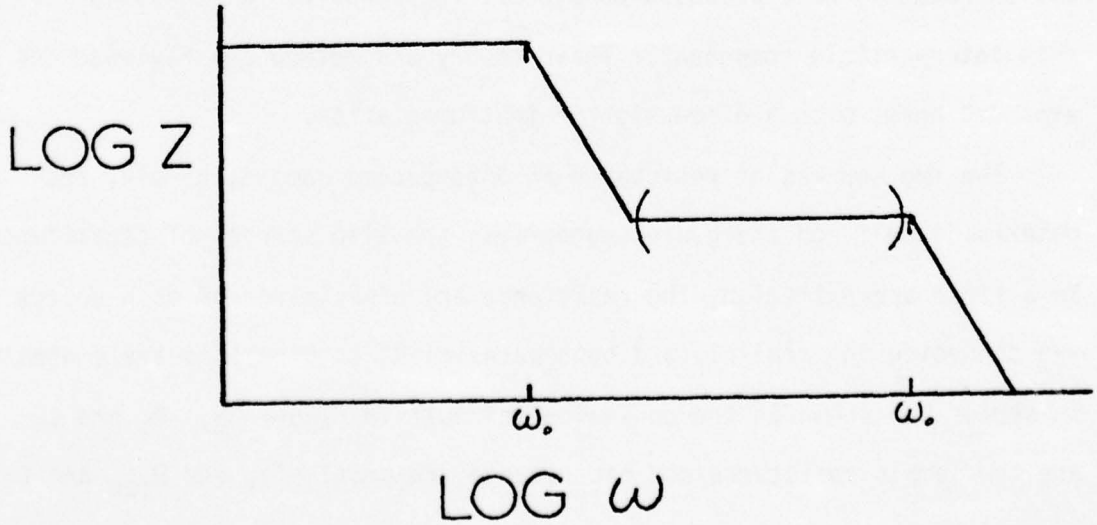

FIGURE 3c. Idealized Bode Plot for Two Parallel RC Circuits in Series

are the interparticle contact resistance and capacitance, respectively. A d.c. current flowing through this circuit sees only the two resistances, but the situation is different for alternating current, which sees the capacitance as well. The capacitive reactance $X_C = \frac{1}{\omega C}$ and the resistance in each RC loop couple vectorially to generate an impedance which is frequency dependent. Impedances in series are additive, so the measurement voltage/current for a compacted sample is the sum of the impedances from each source.

The complex impedance in each RC loop is given by the equation

$$|Z| = \frac{R}{1+j\omega RC}$$

where $j = \sqrt{-1}$ and ω is the angular frequency of the current, which is derived from the addition law of parallel impedances. This equation requires that the impedance must decrease (roll off) in magnitude as the frequency is increased. An idealized Bode plot of log Z versus log ω is shown in Figure 3b. The break point is determined by a time constant $\tau = RC$, which corresponds to a frequency $\omega_o = \frac{1}{\tau} = \frac{1}{RC}$.[16] It should be noticed that the plot is approximately horizontal out to ω_o i.e. from zero to ω_o, Z is approximately equal to R.

For two parallel RC loops in series, as required for a compacted sample, the impedance measured is the sum

$$Z(\text{total}) = Z_1 + Z_2 = \frac{R_1}{1+j\omega R_1 C_1} + \frac{R_2}{1+j\omega R_2 C_2} .$$

The two impedances roll off independent of each other, each responding to its characteristic time constant. The impedance with the larger time constant

rolls off at a lower ω_0. If the time constants are many orders of magnitude different, the log Z versus log ω plot shows two well-resolved roll-off curves, as in Figure 3c.

The impedance at ω equal to zero is R_1 plus R_2. If R_1C_1 is much greater than R_2C_2, the horizontal portion of the curve between the break points (enclosed in parenthesis in Figure 3c) is equal to R_2; similarly, for R_2C_2 much greater than R_1C_1, the horizontal portion is equal to R_1.

Now let $R_1 = R_s$, $C_1 = C_s$, $R_2 = R_{ipc}$, and $C_2 = C_{ipc}$. Huggins and Sharbaugh[17] made the assumption that R_{ipc} was larger than R_s and that C_{ipc} was much larger than C_s, with the result that the interparticle contact impedance rolls off at low frequencies, leaving the impedance intrisic to the material to roll off at high frequencies. This can be understood in terms of the time constants. Thus, if the frequency of the alternating current course is scanned out to high frequencies and two well-resolved roll-off curves can be obtained, the curve at higher frequencies should correspond to the single crystal impedance. The single crystal resistance can be easily obtained from the graph by extrapolating from the horizontal portion between the break points to the y-axis.

This graphical analysis will not be possible if the time constants are similar and the roll-off curves overlap. In support of the assumptions, Wheland and Gillson have reported that compacted sample resistivities averaged two orders of magnitude greater than single crystal values for highly conducting charge-transfer complexes.[18]

In terms of instrumentation, two ways of evaluating the single crystal resistance were investigated: by alternating-current Wheatstone bridge, and by an alternating current source in conjunction with an a.c. voltmeter.

Neither method is without its problems, usually because instruments with loss-free response over a wide range of frequencies are not routinely available. It is estimated that a bandwidth of zero to 10^6 Hertz is desirable as a starting figure. Thus, instrumentation must be carefully chosen.

It was not possible to perform bridge measurements on the complexes characterized in this project, since the only available bridge (a General Radio Type 1615-A Capacitance Bridge) would not measure resistances below ten kiloohms, but a description of the measurement is given below for reference. A schematic of the bridge circuit is shown in Figure 4. An a.c. voltage source is used to power the bridge. R_1 and R_2 essentially control the gain of the instrument. The crucial elements are R_3 and C, connected in parallel to match the sample network, which are variable components adjusted by decade switches. S is the sample and N is the null detector. The measurement consists of minimizing the null detector reading by adjustment of R_3 and C. At this point, the value of R_3 represents the equivalent resistance of the sample. Over a range of frequencies, R_3 will vary between $R_s + R_{1pc}$ at low frequencies to R_s at high frequencies, if the assumptions above hold true.

Attention was then turned to impedance measurements $(\frac{V}{I})$, with the hope of designing a system with a frequency band width extending out to the megahertz range. The proposed electrical network is shown in Figure 5a with connections for a two-probe measurement. A summary of the efforts expended toward this end are included here so that future workers will benefit from this experience.

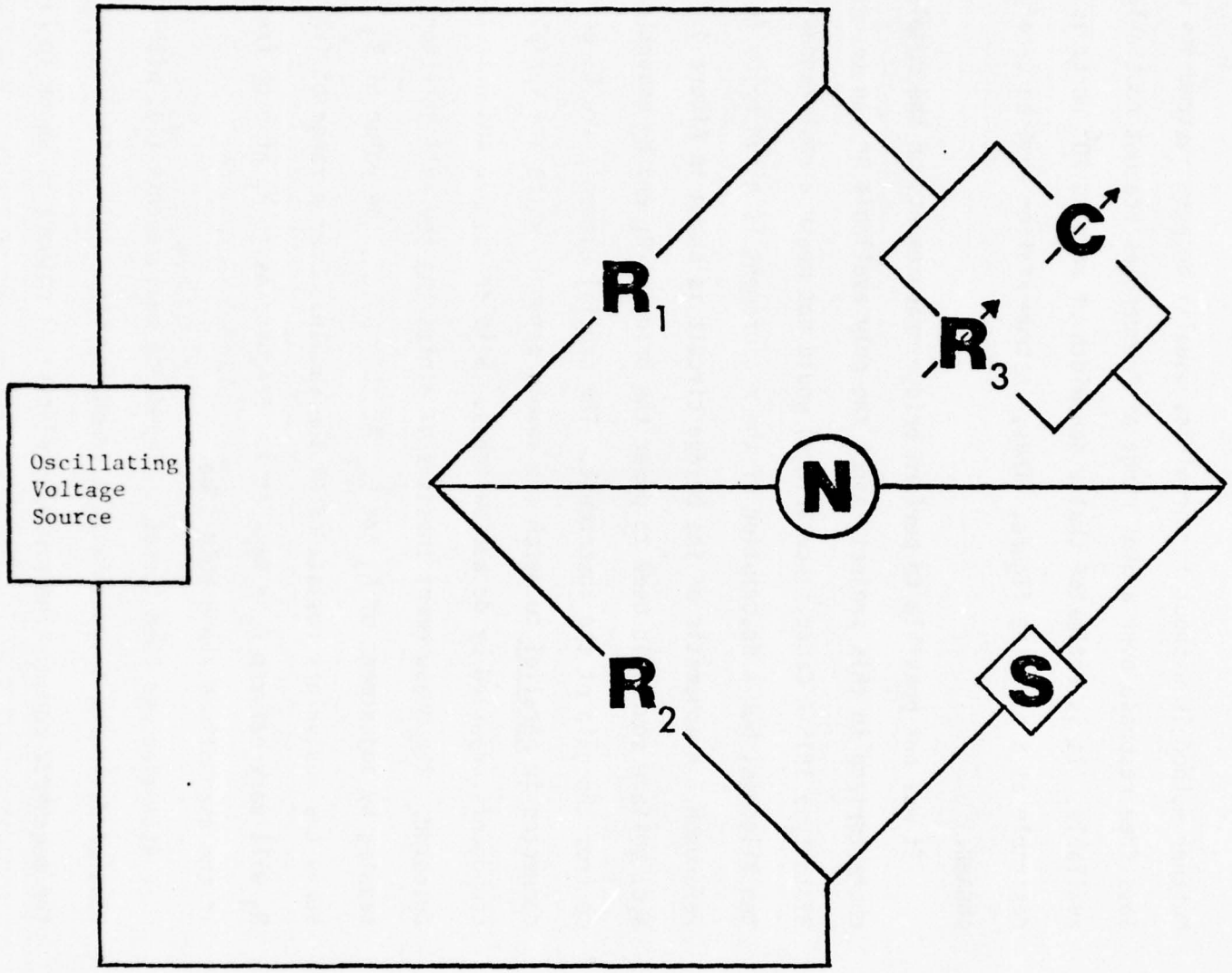

FIGURE 4. Alternating-current Wheatstone Bridge for Measuring Equivalent Resistance

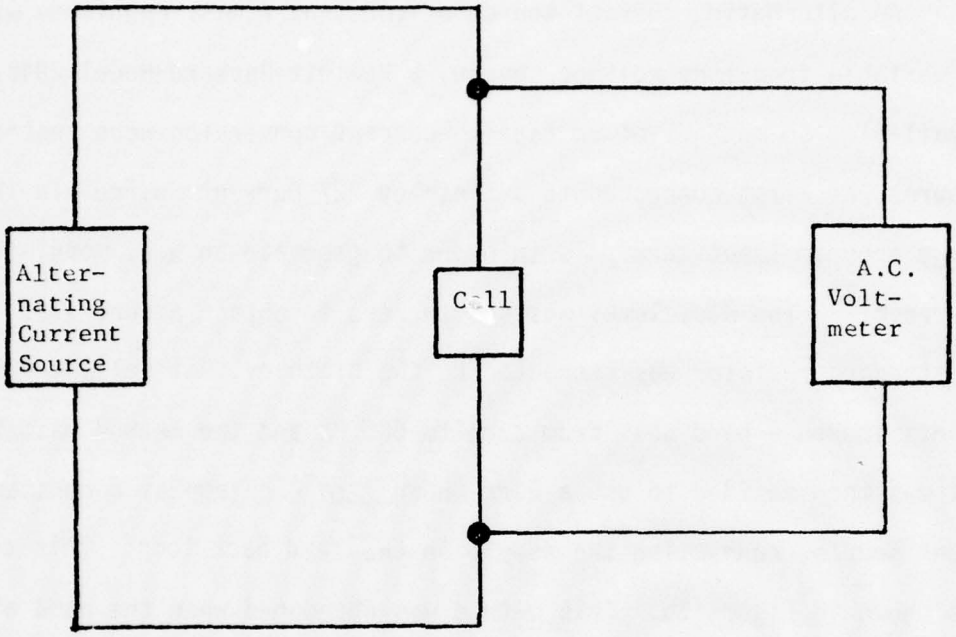

FIGURE 5a. Circuit for 2-Probe
Impedance Measurement

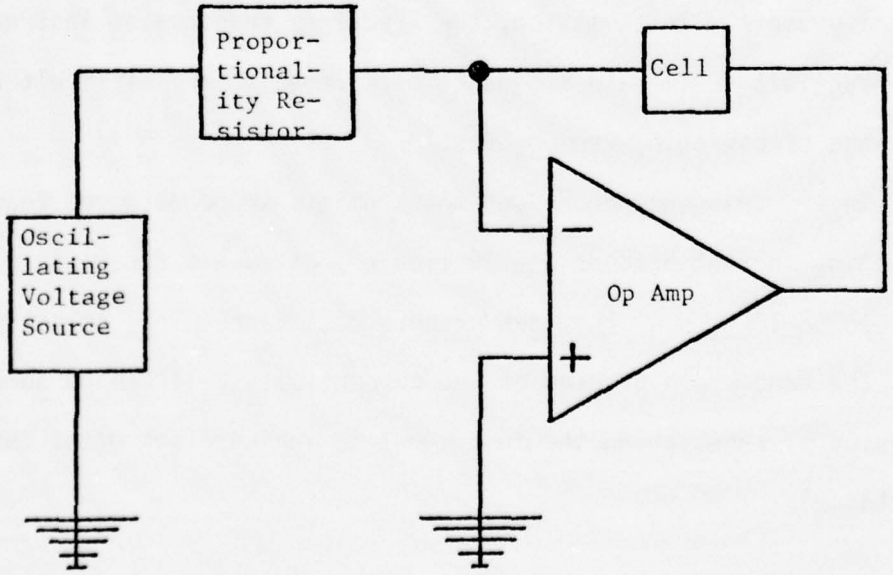

FIGURE 5b. Controlled Current Source
using Op Amp for Impedance Measurement

An alternating current source of constant r.m.s. magnitude was needed. A variable frequency voltage source, a Hewlett-Packard Model 204C, was available, so methods of voltage-to-current conversion were tested. The source was first connected to a Kiethley 227 Current Source via the voltage program input terminals in order to generate an a.c. modulated d.c. current.[19] The d.c. level was set to zero to obtain a pure a.c. current. A standard resistor was connected to the Kiethley, but voltmeter measurements showed a band pass from zero to 600 Hz and the method was abandoned. It was then decided to use a Burr-Brown 3507 J op amp as a constant current source, connecting the sample in the feed back loop. This circuit is shown in Figure 5b. This method was abandoned when the band width proved to be 10^2 to 10^5 c.p.s. This was attributed to the band width of the a.c. voltmeter. In addition, there is a limiting band pass associated with the conductivity cell, which is high in capacitance due to the volume of metal present. In summation, the frequency response of instruments and conductivity cell make impedance measurements very difficult over a wide range of operating frequencies.

However, frequency-dependent measurements are considered feasible. Alternating-current bridges are available that have a frequency response from zero to 10^6 c.p.s. that can measure resistances less than ten kilohms. The band width problem of the conductivity cell can be somewhat alleviated by redesigning the instrument to include less metal (hence less capacitance).

Room Temperature Resistivity Measurements

The room temperature (25°C) resistivities of each of the complexes reported in Table 1 are recorded in Table 3. The measurements were made

TABLE 3

Room Temperature Resistivities

(ohm-cm)

Resistivities of DAAQ + Acceptors

donor/acceptor	$CuCl_2$	$CuBr_2$	I_2
1,2-DAAQ	$>10^7$	$>10^7$	-
1,4-DAAQ	8.3×10^3	3.5×10^3	1.2×10^2
1,5-DAAQ	$>10^7$	-	$>10^7$

Resistivities of 1,4-DAAQ·I_2 System by Stoichiometry:

2:1	2.5×10^3
1:1	1.2×10^2
2:3	2.5×10^3
1:2	4.8×10^3

Other Resistivities:

Sample	
phenothiazine·I_2(2:3)	3.6×10^3
1,4-DAAQ(pure)	$>10^7$

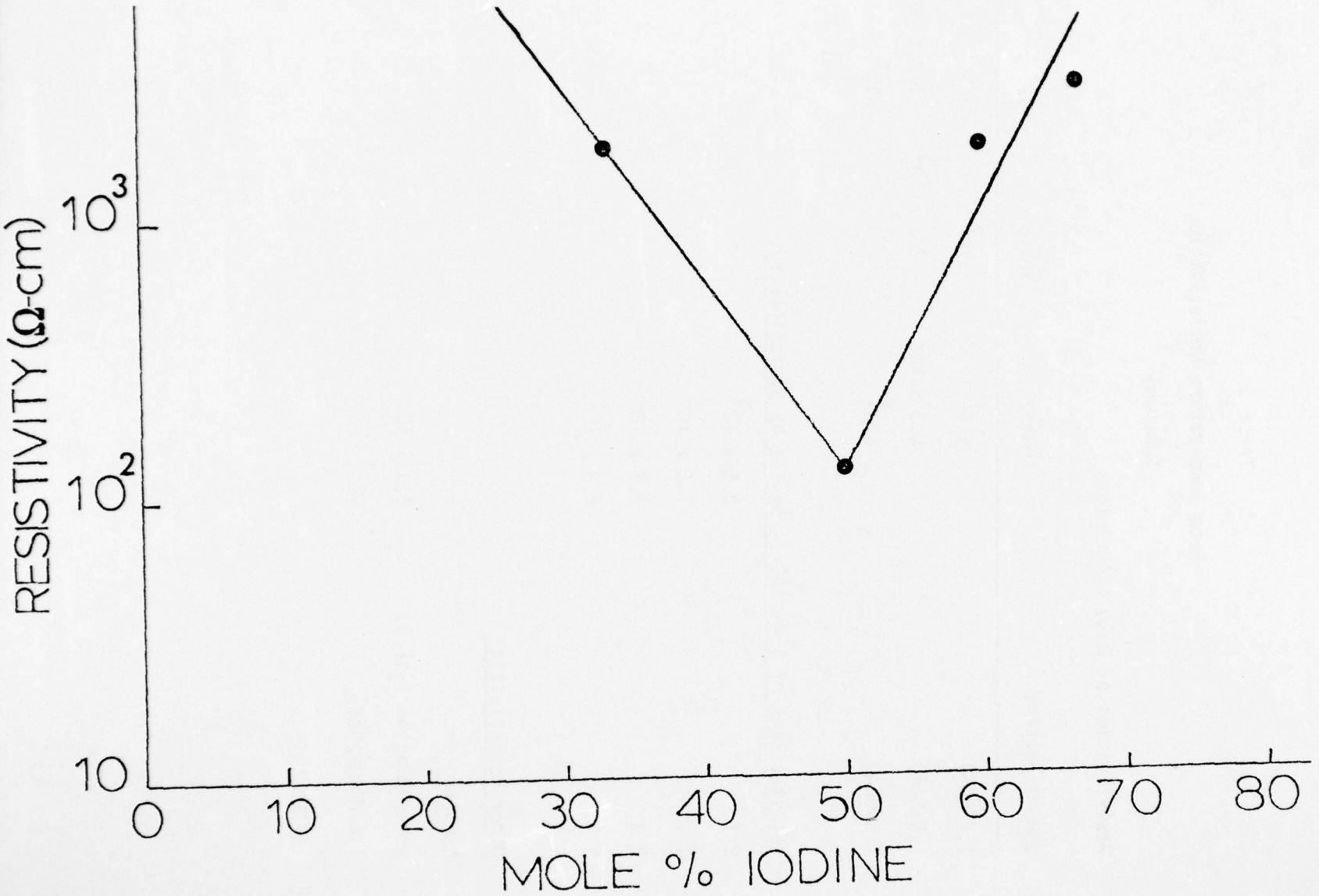

FIGURE 6. Resistivity versus Mole % Iodine for 1,4-DAAQ·I_2 System

using the conductivity cell described above with d.c. current. The most significant feature of these data is that the complexes 1,4-DAAQ·I_2 and 1,4-DAAQ·CuX_2 (X = Cl,Br) show relatively low resistivities of 10^2 to 10^3 ohm-cm, whereas the complexes 1,2-DAAQ·CuX_2, 1,5-DAAQ·I_2, and 1,5-DAAQ·$CuCl_2$ are poorer semiconductors or insulators with resistivities above 10^7 ohm-cm. It has therefore been determined that use of the donor molecule 1,4-diaminoanthraquinone leads to relatively high conductivity, whereas 1,2- and 1,5-diaminoanthraquinone are ineffectual in this regard. To validate these results, the room temoerature resistivity of pure 1,4-DAAQ was measured and found to be greater than 10^7 ohm-cm.

Resistivity data for the 1,4-DAAQ·I_2 system over the stiochiometry range 1:2 to 2:1 are plotted in Figure 6. It is noted that the 1,4-DAAQ·I_2 complex shows a minimum in resistivity at the stoichiometry 1:1. Gutmann and Keyzer[20] have found that the phenothiazine:I_2 system shows a resistivity minimum at 2:3 stoichiometry.

Another interesting aspect of these results is that 1,4-DAAQ forms complexes with both iodine and copper(II) that do not differ greatly in resistivity, even though these acceptors differ greatly in acceptor strength and chemistry. Molecular iodine has the higher standard reduction potential, +0.53 volts, and has no coordination chemistry, whereas copper(II) shows a smaller one-electron standard reduction potential of +0.15 volts and can readily coordinate 1,4-DAAQ via the amino and carbonyl groups. By extension of past findings,[21] it is easy to postulate that crystalline 1,4-DAAQ·I_2 should contain segregated stacks of planar 1,4-DAAQ molecules in a matrix of polyiodide species, and that these stacks are one-dimensional

pathways for electronic conduction, as shown in Figure 7. However, an equivalent structure cannot be easily postulated for 1,4-DAAQ·CuX_2 (X = Cl, Br) in the solid state because 1,4-DAAQ surely coordinates to the copper ion. A probable structure is shown in Figure 8 where a linear chain of [Cu(1,4-DAAQ)X_2] repeating units is suggested. The amino and carbonyl groups are predicted to form square planar coordination about copper(II) with two halides occupying the axial positions. This is a good assumption for the 1:1 1,4-DAAQ·$CuCl_2$ complex, but the 3:2 1,4-DAAQ·$CuBr_2$ complex requires additional explanation in that an additional 1,4-DAAQ molecule per every two repeating units must be accounted for. The best explanation is probably intercalation of additional 1,4-DAAQ molecules between adjacent linear chains. It is difficult to postulate a conducting pathway for these copper complexex without crystallographic data and this will not be attempted. The point is that entirely different structures must be postulated for the copper and iodine complexes.

Electrical Characterization

The electrical properties of crystalline materials depend on the width of the energy gap ΔE between the valence and conduction bands according to band theory.[22] Insulators have prohibitively large energy gaps. Semiconductors show lesser gaps, and metals show zero band gaps. In intrinsic semiconductors, electrons are promoted from the valence band to the conduction band by whatever energy is available, where they participate in conduction. The ratio of the number of electrons in the conduction band to the number in the valence band follows the Boltzmann distribution, and from this the conductivity, σ, as a function of temperature (T) has been

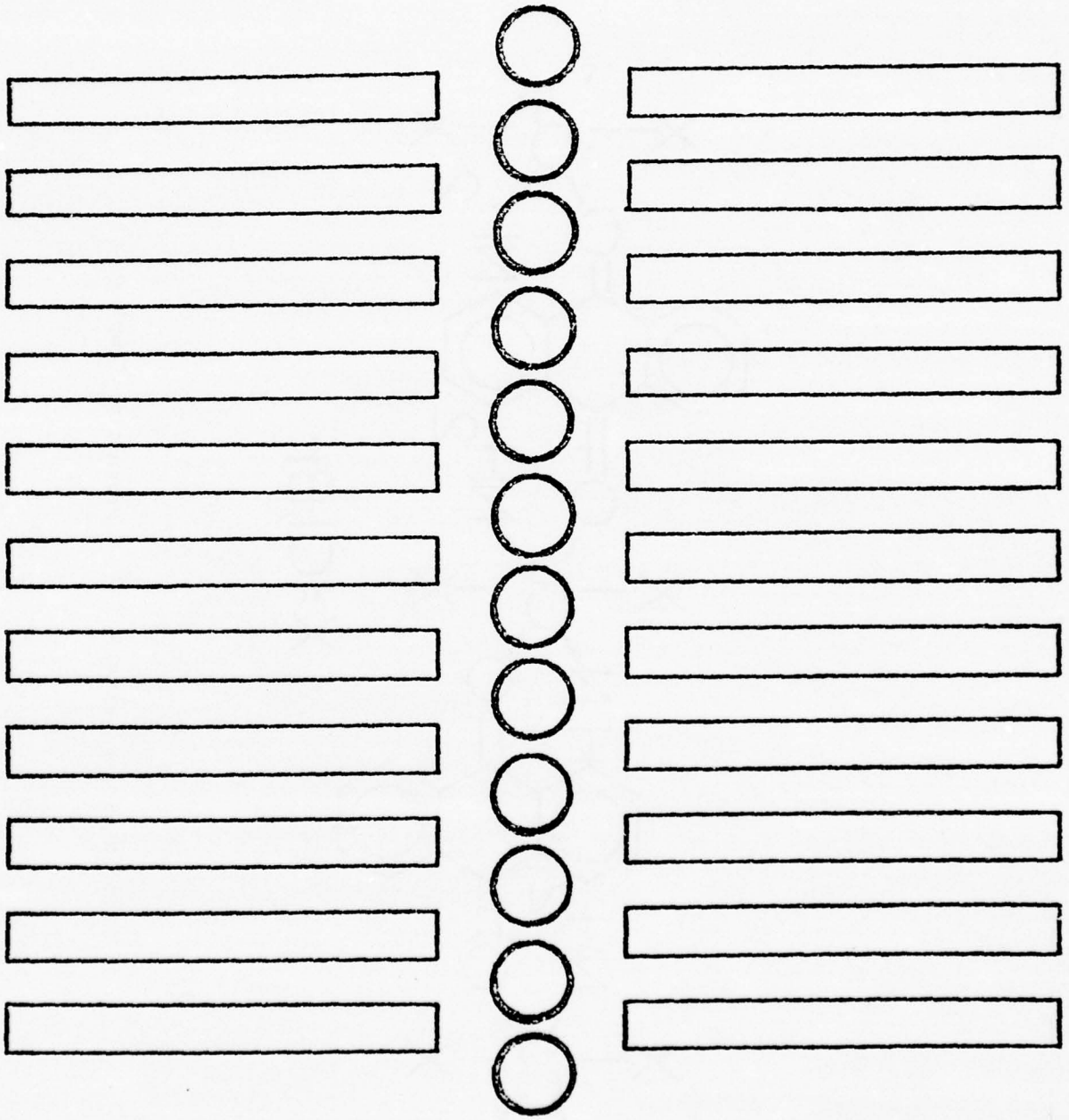

FIGURE 7. 1,4-DAAQ·I_2 Charge-Transfer Complex. View is perpendicular to the axis of stacking. The center column represents a polyiodide chain, while the outside columns represent stacks of 1,4-DAAQ molecules.

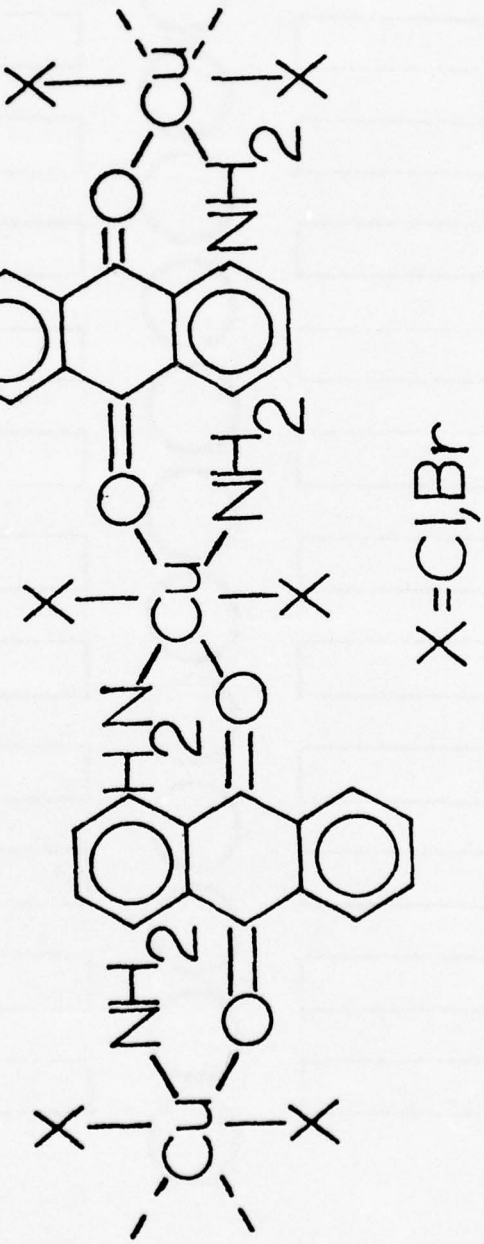

FIGURE 8. 1,4-DAAQ + CuX_2 Coordination Complex

shown[23] to be

$$\sigma(T) = \sigma_0 \exp(-\Delta E/kT)$$

where σ_0 is a preexponential constant and k is the Boltzmann constant. This equation can be rewritten in terms of resistivity to become the following

$$\rho(T) = \rho_0 \exp(+\Delta E/kT)$$

where ρ_0 is a preexponential constant.

The conductivity of a semiconductor is therefore expected to increase as temperature increases. Metals also show a temperature dependent behavior, but here the conductivity decreases as temperature increases due to thermally activated lattice vibrations which disrupt the periodic positive potential through which conduction electrons pass (lattice scattering). It is therefore possible to classify an unknown material from the temperature dependence of its conductivity: a semiconductor will show zero conductivity at absolute zero and a positive temperature coefficient of conductivity $d\sigma/dT$, whereas a metal will show a non-zero conductivity at absolute zero and a negative $d\sigma/dT$. Some materials however, show both behaviors in different temperature regions, with the transition in behavior usually accompaning a structural phase transition.[24]

The band gap ΔE may be determined from temperature dependent conductivity (or resistivity) data by plotting the natural logarithm of resistivity versus the reciprocal temperature. If the plot is linear, then the band gap can be calculated from the slope of the line by the relation

$$\text{slope} = \frac{\Delta E}{K}$$

In theory, the band gap can also be determined from absorption spectroscopy. Electronic transitions can occur between the top of the valence band and virtually any energy within the conduction band, so a broad electronic absorption band is to be expected, the width depending on the width of the conduction band. The point of interest here, i.e. the band gap energy, is the lowest energy necessary to promote an electron. This is found at the low energy edge of the absorption band and is accordingly called the absorption edge. Optical promotion of valence electrons into the conduction band is known as photoconductivity.

In practice, it is easier to calculate the activation energy initially from variable-temperature resistivity data, then attempt to verify its existence via absorption spectroscopy.

To put the resistivity measurements contained herein in perspective, it should be noted that the metallic elements copper, silver, gold, and aluminum show resistivities on the order of 10^{-6} ohm-cm. The intrinsic semiconductor germanium shows a resistivity of 10^{1} ohm-cm,[25] while most molecular crystals have values between 10^{10} and 10^{14} ohm-cm.[26]

Variable-Temperature Resistivity Measurements

The resistivities of 1,4-DAAQ·I_2 (2:3), 1,4-DAAQ·$CuCl_2$(1:1), 1,4-DAAQ-$CuBr_2$(3:2) and PH·I_2 (2:3) were measured as a function of temperature between 77°K and 280°K using the procedure and apparatus described above. Plots of conductivity versus temperature are shown in Figures 9 and 12 and plots of ln(resistivity) versus 1/T are shown in Figures 13 and 16.

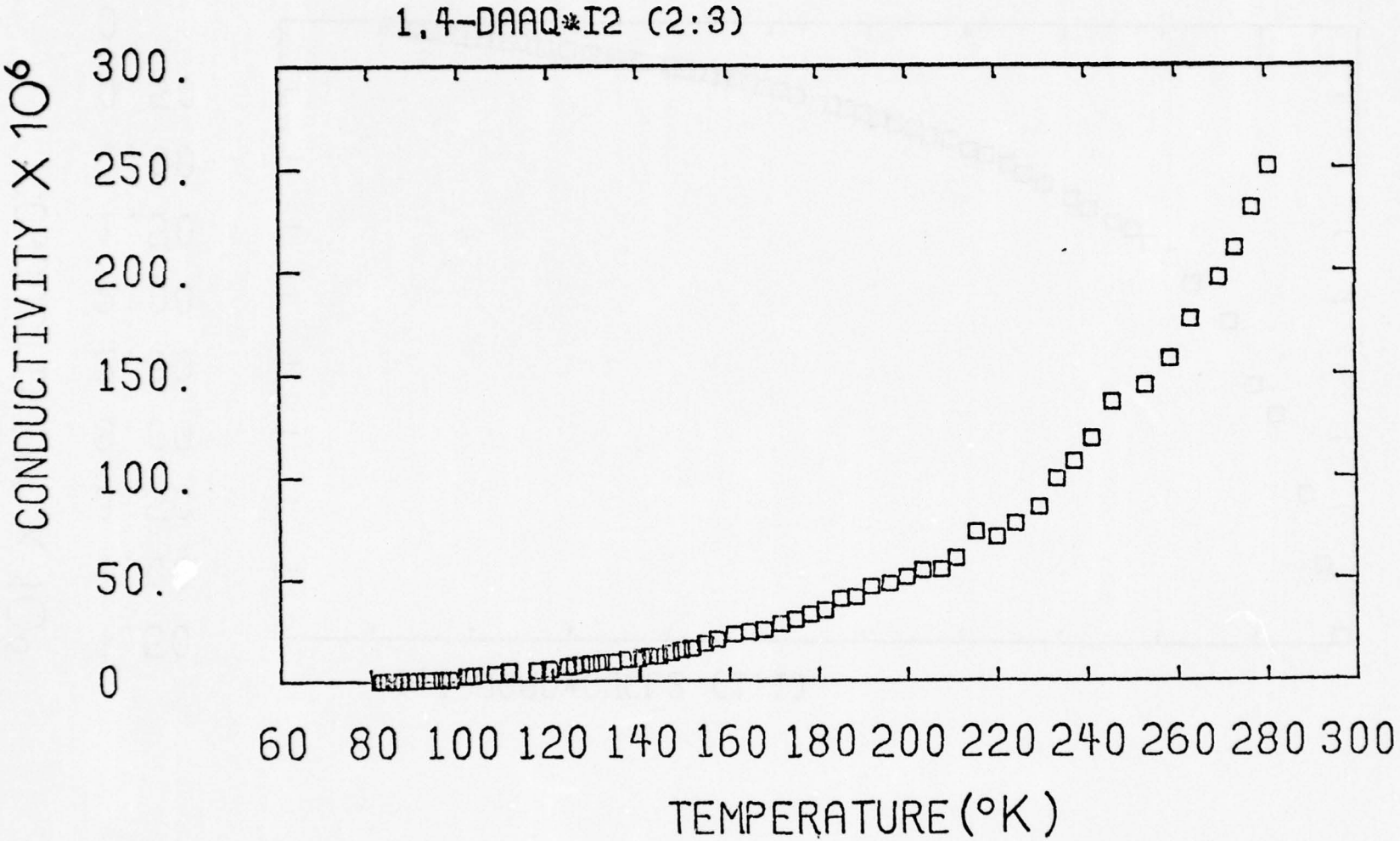

FIGURE 9. Conductivity x 10^6 $(ohm\text{-}cm)^{-1}$ versus Temperature for 1,4-DAAQ·I_2 (2:3)

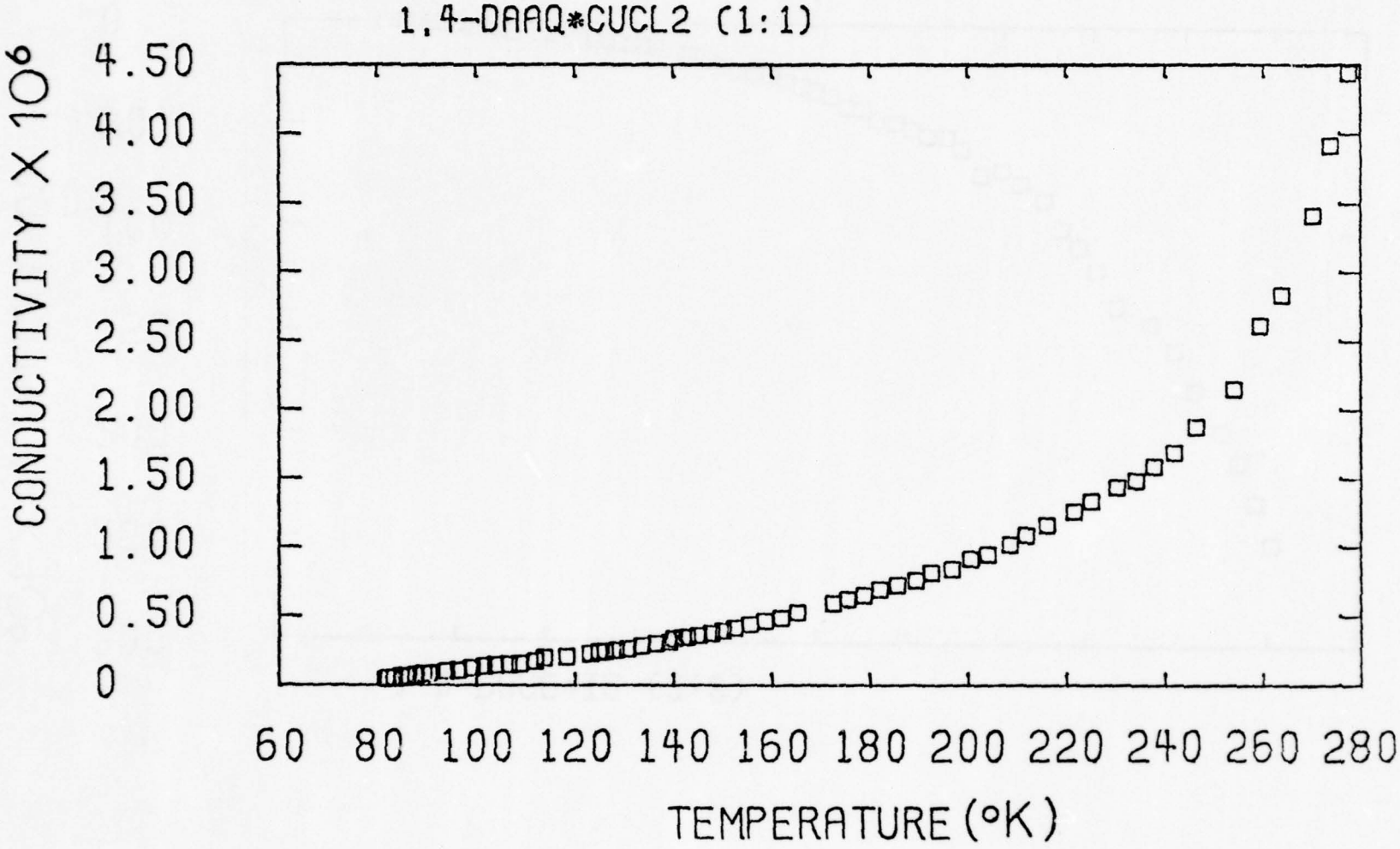

FIGURE 10. Conductivity x 10^6 $(ohm\text{-}cm)^{-1}$ versus Temperature for 1,4-DAAQ·$CuCl_2$ (1:1)

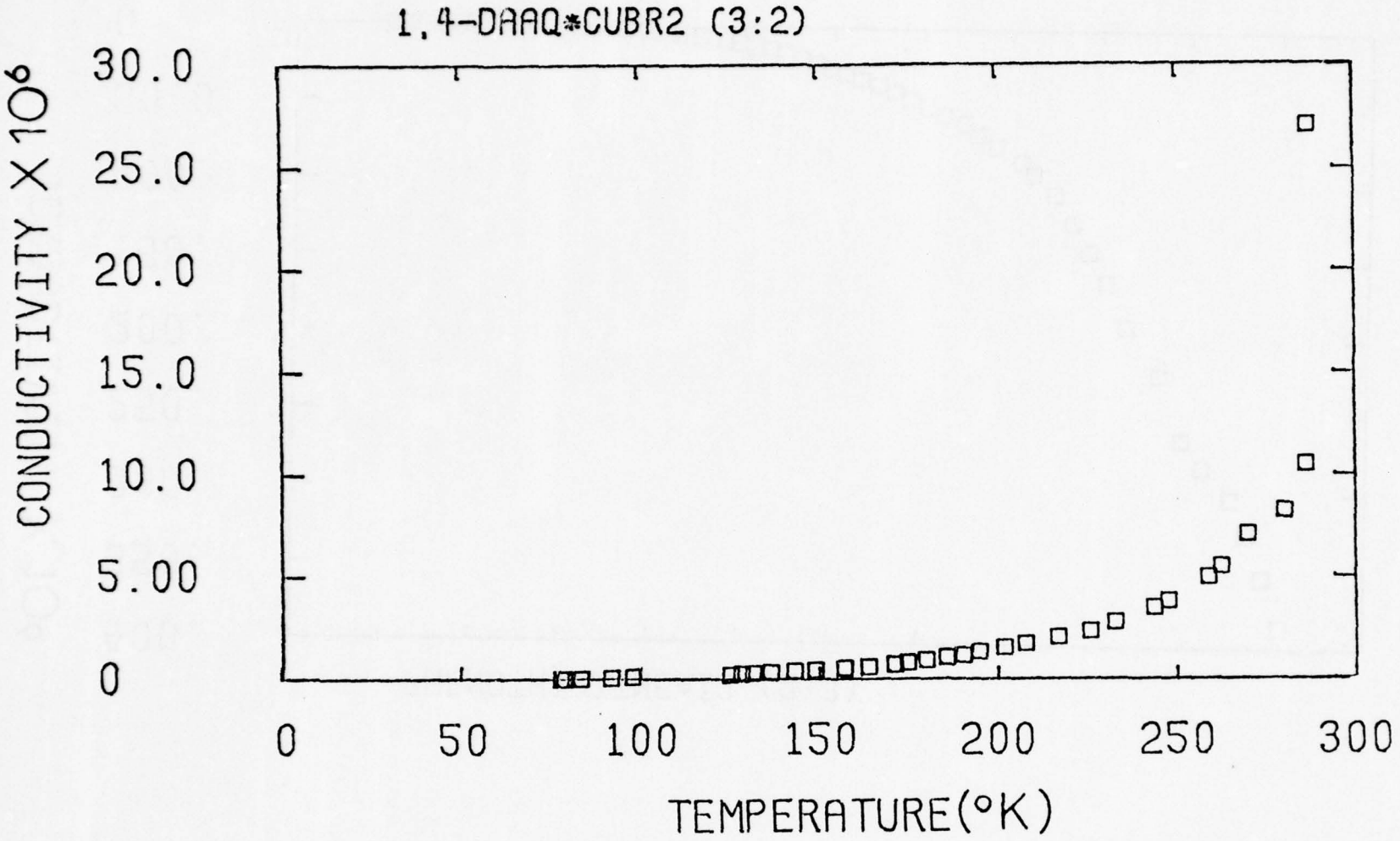

FIGURE 11. Conductivity x 10^6 $(ohm\text{-}cm)^{-1}$ <u>versus</u> Temperature for 1,4-DAAQ·$CuBr_2$ (3:2)

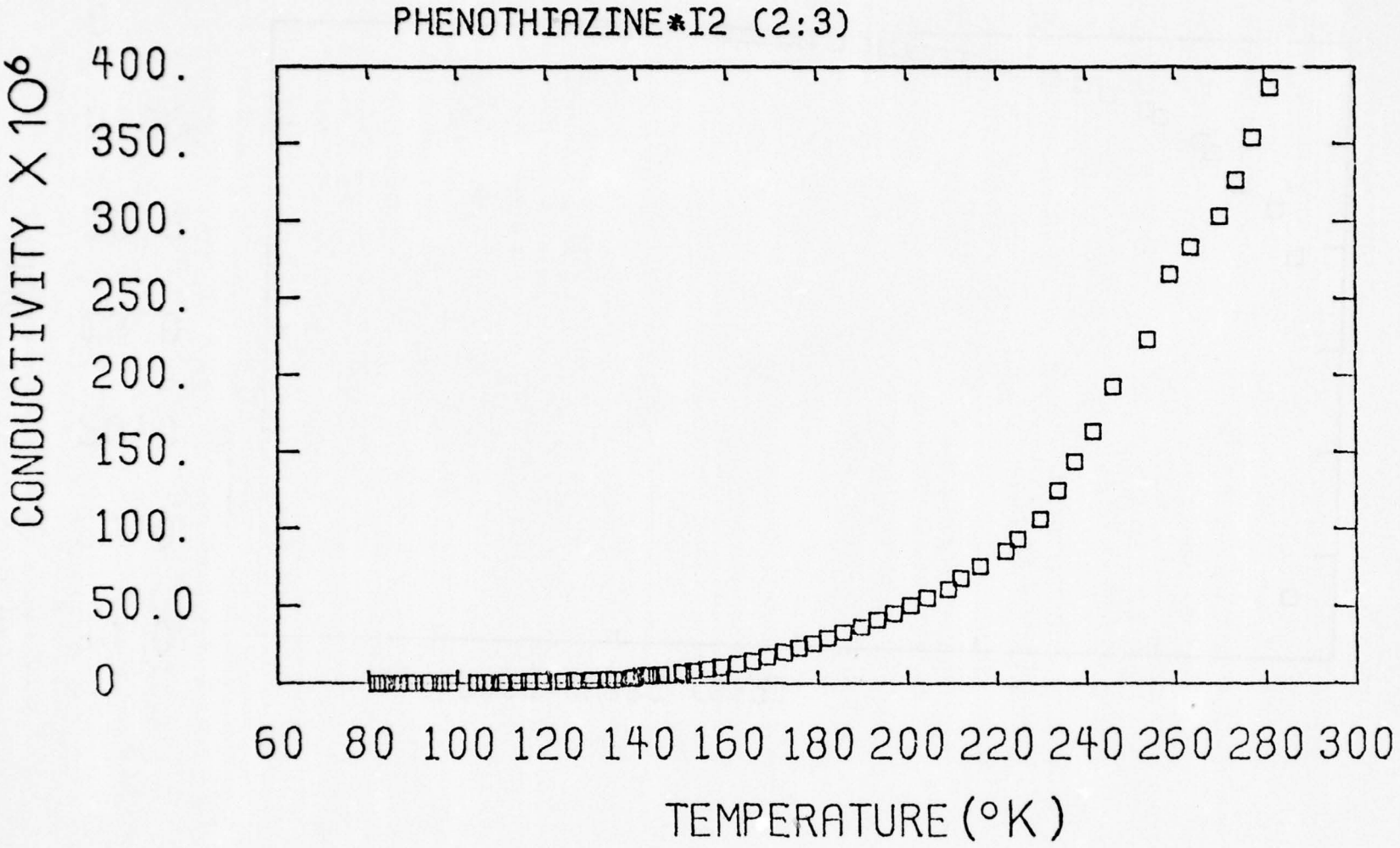

FIGURE 12. Conductivity x 10^6 $(ohm\text{-}cm)^{-1}$ versus Temperature for Phenothiazine·I_2 (2:3)

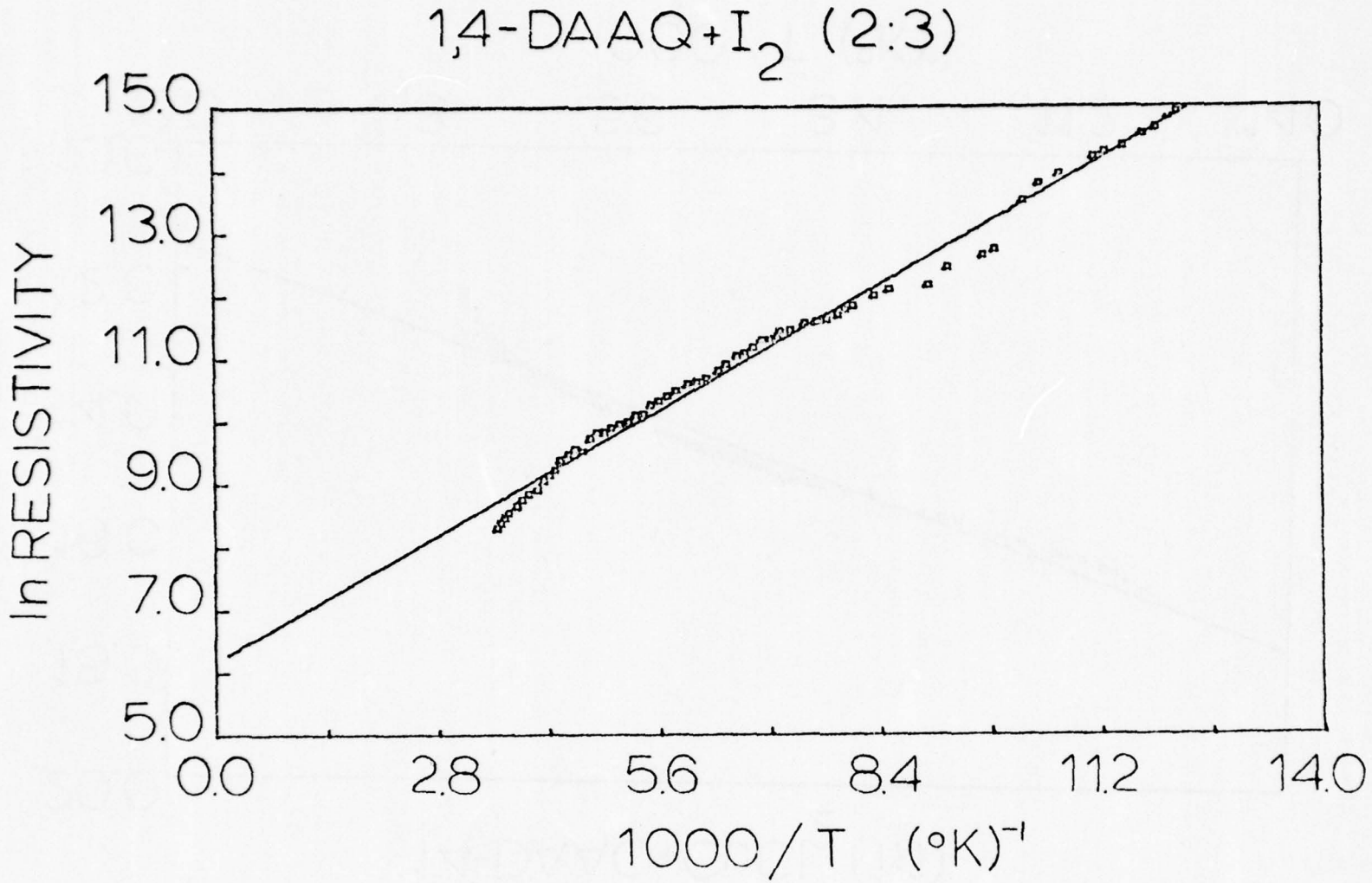

FIGURE 13. ln(Resistivity) versus 1000/T for 1,4-DAAQ·I_2 (2:3)

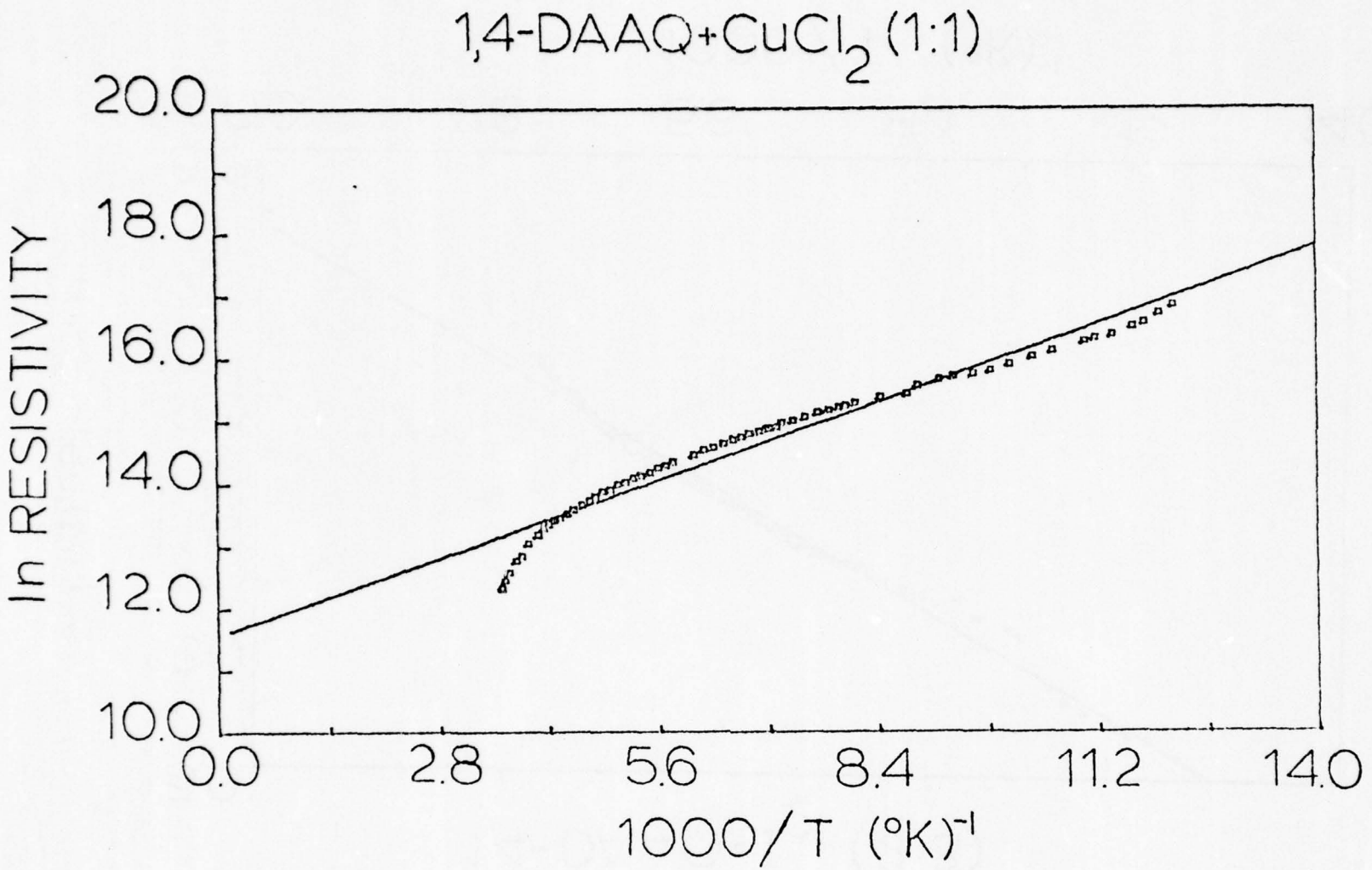

FIGURE 14. ln(Resistivity) versus 1000/T for 1,4-DAAQ·$CuCl_2$ (1:1)

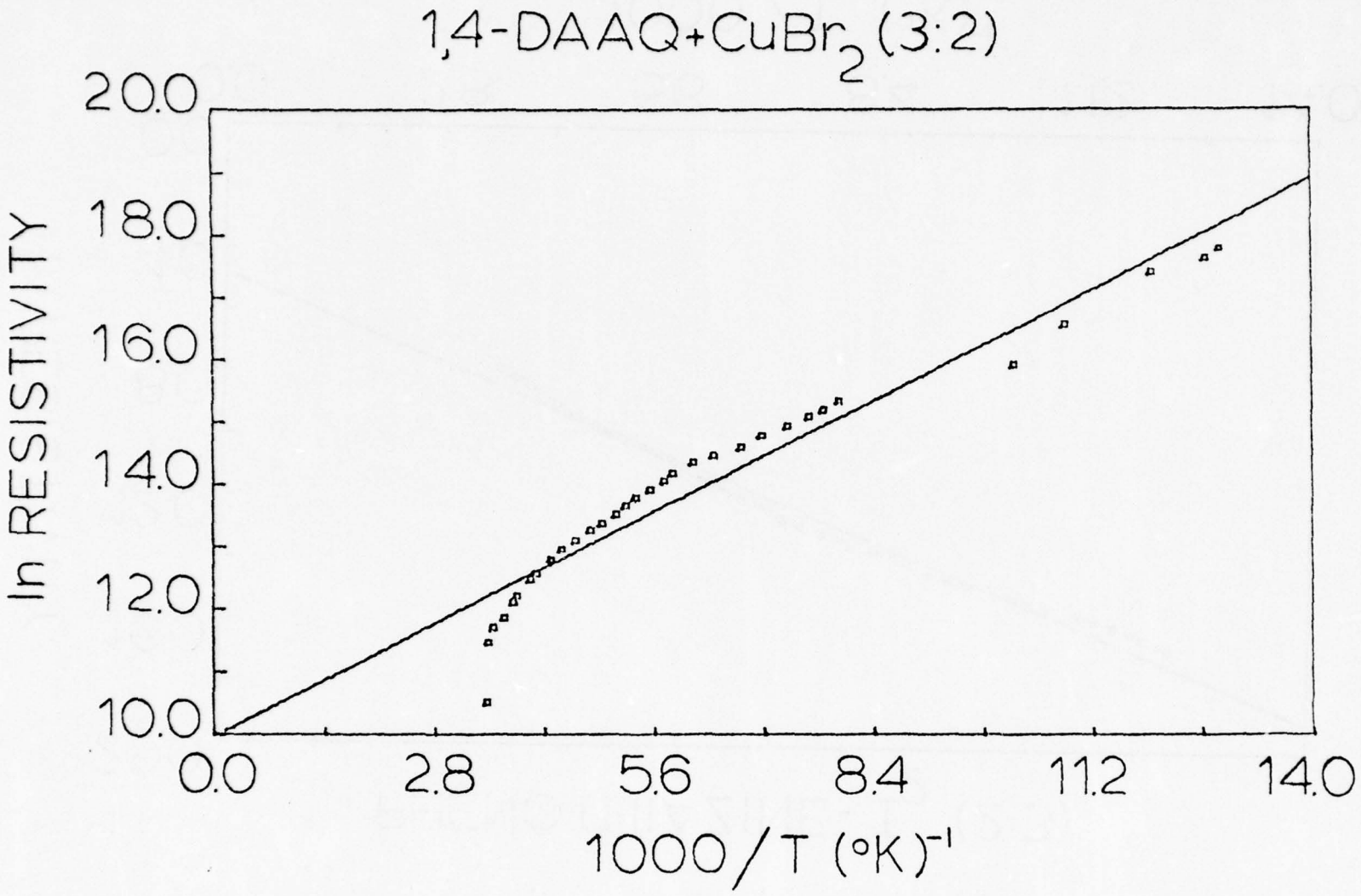

FIGURE 15. ln(Resistivity) versus 1000/T for 1,4-DAAQ·$CuBr_2$ (3:2)

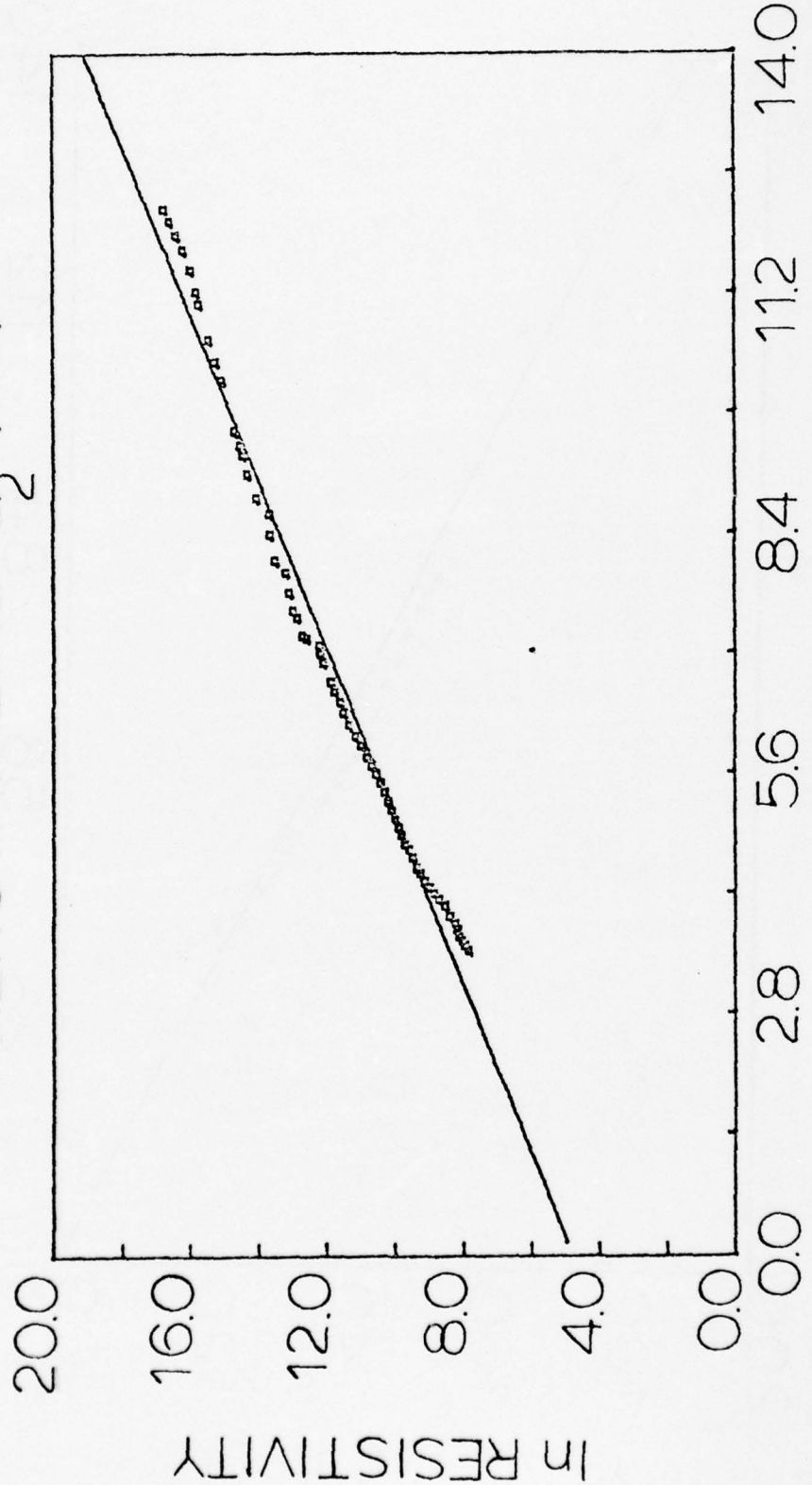

FIGURE 16. ln(Resistivity) versus 1000/T for Phenothiazine·I_2 (2:3)

All complexes without exception show temperature dependent conductivity over the entire region 77°K to 280°K. The positive slope $d\sigma/dT$ indicates that the complexes are all semiconducting. The plots of ln(resistivity) *versus* 1/T are basically consistent with the following conduction mechanism: one conduction band being expotentially populated as a function of temperature (intrinsic semiconduction). Small deviations from linearity are observed, however, especially at higher temperatures. Possible explanations for these deviations are: 1) Temperature-dependent structural transitions which change the activation energy may be occurring. The curvature of some plots suggest continuous structural change,which has been observed before.[27] 2) Impurities may be present in the solid state lattice which create additional conduction levels that may be populated expotentially (extrinsic semiconduction).

A statistical analysis of these deviations is presented in Table 4, which reports the experimental linear-correlation coefficient,[28] defined as $R = (b \cdot b')^{1/2}$ when b = slope of y(x) and b' = slope of x(y). Here y = ln(resistivity) and x = 1/T. An R value of one is indicative of a completely linear correlation of y to x, while a value of zero indicates no correlation. The percent deviations from 1.000 are largest for the copper(II) halide adducts of 1,4-DAAQ, indicating that these complexes deviate most from intrinsic semiconduction.

Table 4 also reports the experimentally determined activation energies, obtained from the slope of ln(resistivity) *versus* 1/T as described above. A least-squares analysis of the data was employed, and the activation energies

TABLE 4

Activation Energies and Linear Analysis

Complex	ΔE(eV)	$\Delta E(cm^{-1})$	R-factor	% deviation (from 1.000)
phenothiazine·I_2(2:3)	0.088	710	0.992	0.8
1,4-DAAQ·I_2(2:3)	0.062	496	0.995	0.5
1,4-DAAQ·$CuCl_2$(1:1)	0.039	311	0.977	2.3
1,4-DAAQ·$CuBr_2$(3:2)	0.055	444	0.966	3.4

are reported both in electron volts and reciprocal centimeters. The following conversions were used:

$$1 \text{ erg} = 6.242 \times 10^{11} \text{ eV}$$

$$1 \text{ eV} = 8066 \text{ cm}^{-1}.$$

Absorption Spectra

To test the hypothesis that electrons can be promoted across the band gap in the conduction band by optical activation, infrared and far-infrared spectra were attempted for the complexes 1,4-DAAQ·I_2(2:3),1,4-DAAQ·$CuCl_2$(1:1), 1,4-DAAQ·$CuBr_2$(3:2), and phenothiazine·I_2(2:3). The infrared spectra were run on a Perkin-Elmer 421 Spectrophotometer from both Nujol mulls and potassium bromide pellets, while the far-infrared were run on a Perkin-Elmer 621 from Nujol mulls. Detailed spectra were impossible to obtain due to an unusually high absorption baseline, but no absorption edges were observed at the frequencies predicted in the previous section or otherwise. The absence of the predicted absorption edge has also been noted by Fitz.[29]

Cyclic Voltammetry

The ability of a molecule to donate an electron to an appropriate acceptor is related to its ionization potential, which is in turn related to its electrochemical oxidation potential.[30] As a general rule, moderately strong donors ($0.1v \leq E_{ox} \leq 0.4v$) form highly conducting charge-transfer complexes with moderately strong acceptors ($0v \leq E_{red} \leq 0.35v$).[31] For example, tetrathiofulvalene is one of the best known donors with an oxida-

tion potential of +0.30 volts versus the saturated calomel electrode, and this donor participates in the most conductive charge-transfer complex known (TTF-TCNQ). Thus, the oxidation potential of the donor is a factor which is related to the resultant conductivity of charge-transfer complexes which are formed from it.

Cyclic voltammetry was used to determine the oxidation potentials of 1,2-, 1,4-, and 1,5-diaminoanthraquinones and their radical cations in acetonitrile. Figures 17 through 19 show the voltammograms. A platinum working electrode was used in conjunction with a saturated calomel reference electrode. Tetra-n-butylammonium hexafluorophosphate (TBAH) was the supporting electrolyte, 0.1 molar in acetonitrile. The voltage sweep rate was 200 millivolts per second.

It was found that 1,4-DAAQ showed the lowest oxidation potential, +0.77 volts, versus +0.95 volts for 1,2-DAAQ and +1.31 volts for 1,5-DAAQ (see Table 5). These results were gratifying because, as shown in Table 3, the 1,4-DAAQ adducts showed the lowest resistivities. A correlation between low resistivity and low oxidation potential has thus been established for this series of donors.

On the basis of its oxidation potential (0.77 volts), it was not expected that 1,4-DAAQ would be as good a donor as TTF(0.30 volts), but the resistivity obtained for 1,4-DAAQ$\cdot I_2$ (1:1) is actually less than that reported for the TTF$\cdot I_2$ complex of identical stoichiometry ($\rho = 10^3$ ohm-cm).[32] This is not too surprising however, for it has been demonstrated that other factors not investigated here, particularly crystal structure and degree of charge transfer, have important effects on conductivity. The findings reported within support the conclusion that donor ability is important, but not the only factor involved for high conductivity.

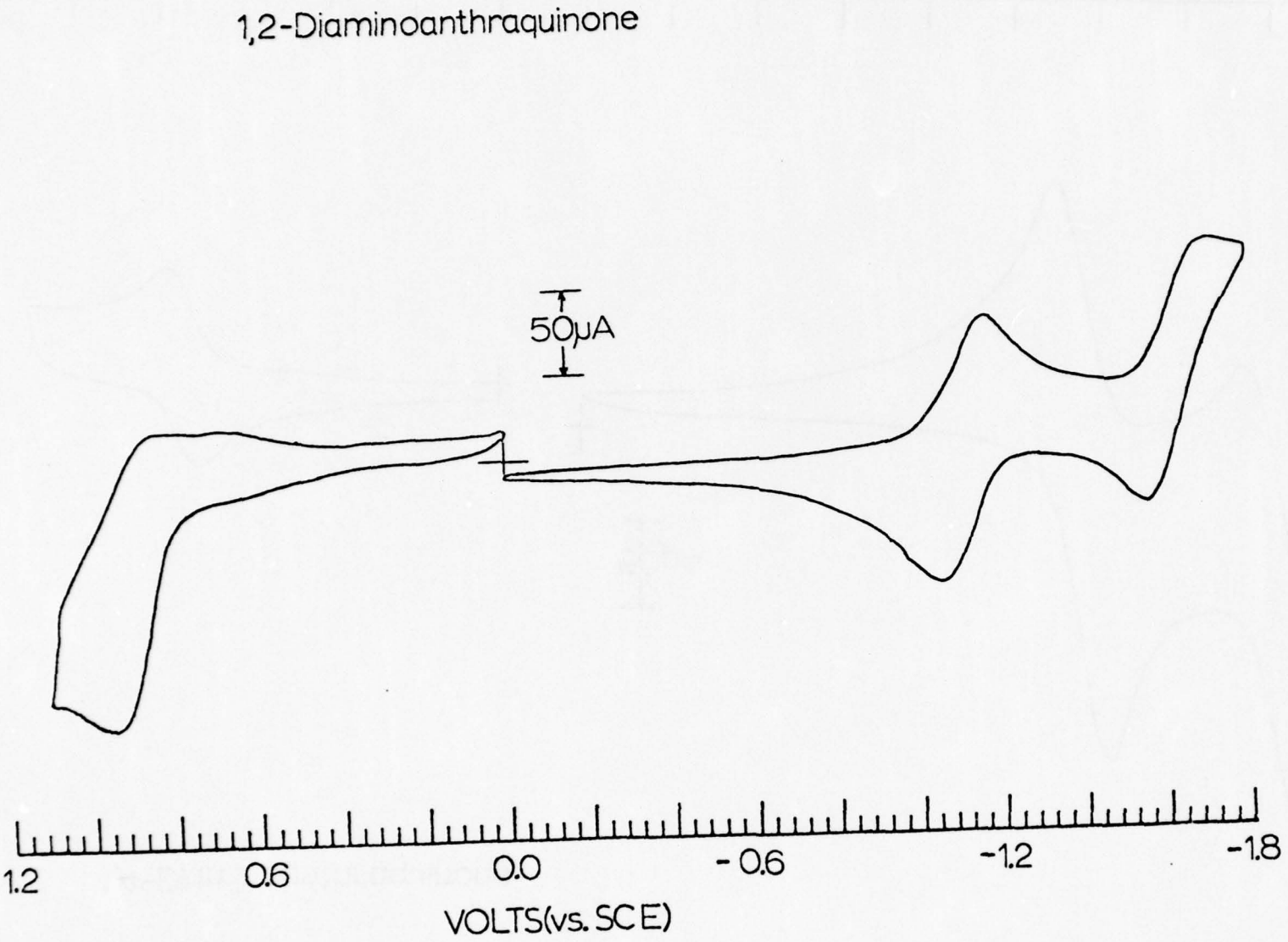

FIGURE 17. Cyclic Voltammogram of 1,2-diaminoanthraquinone

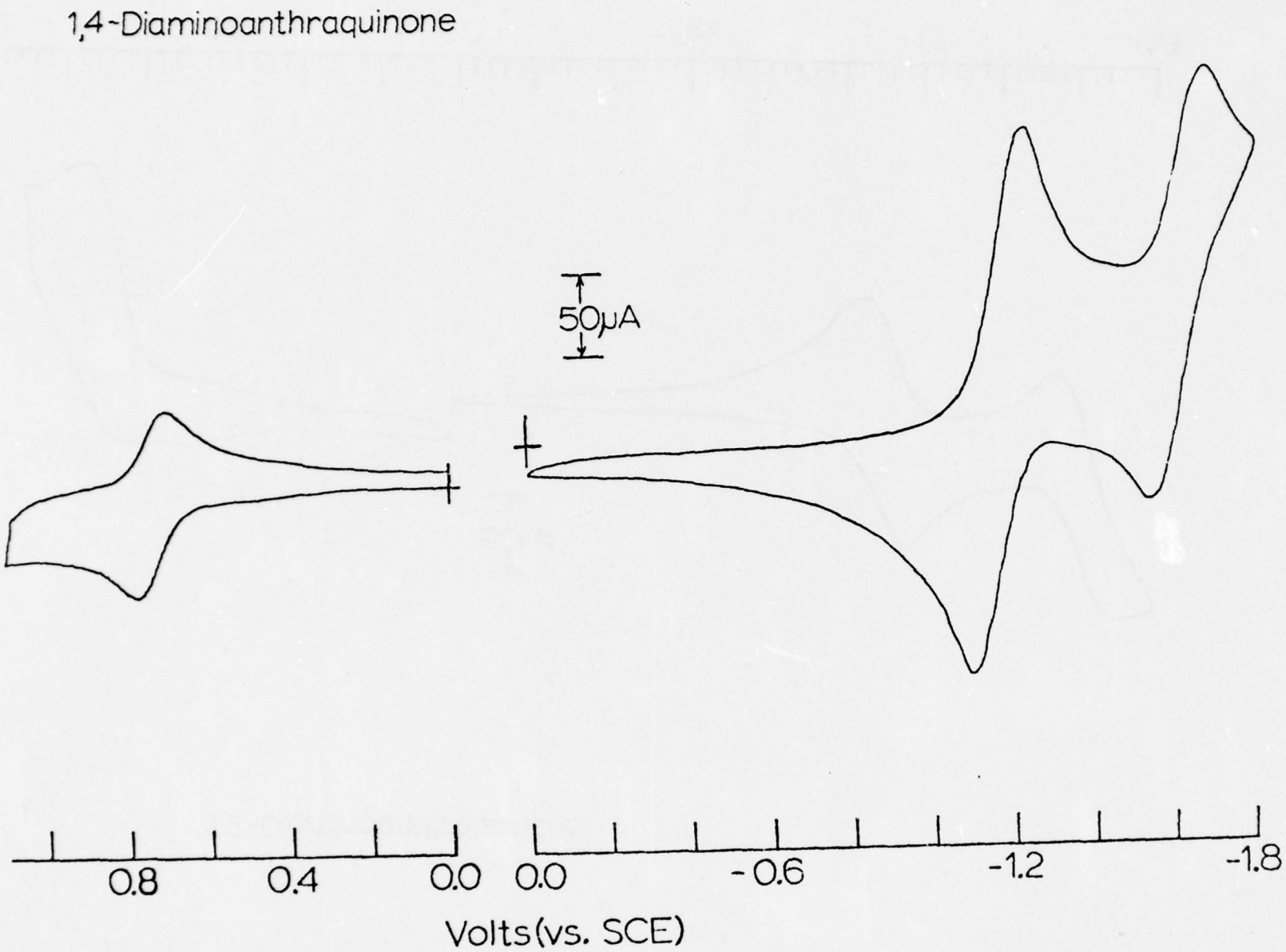

FIGURE 18. Cyclic Voltammogram of 1,4-Diaminoantraquinone

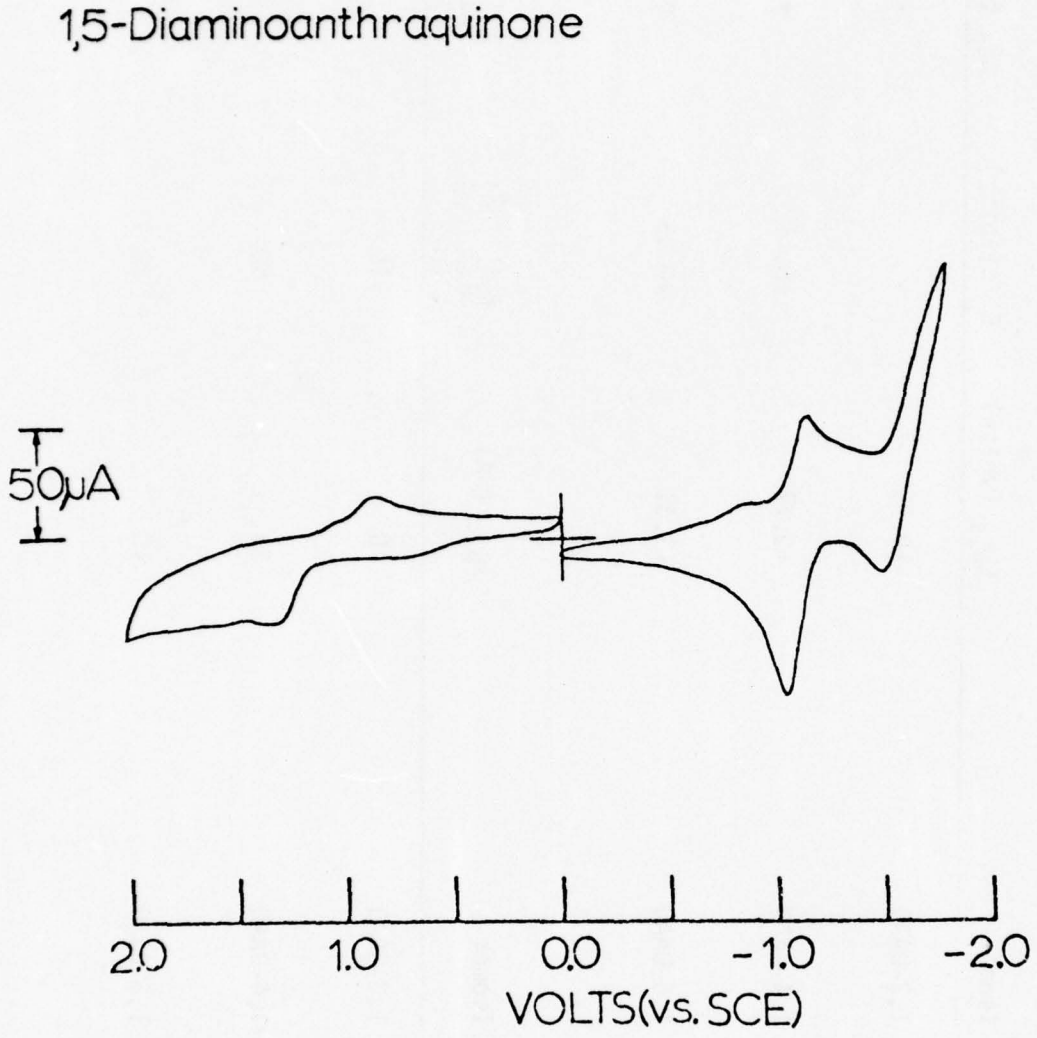

FIGURE 19. Cyclic Voltammogram of 1,5-diaminoanthraquinone

TABLE 5

Analysis of Diaminoanthraquinones by Cyclic Voltammetry

(Oxidation only)

Isomer	$E_{p,a}$ (volts)	$E_{p,c}$ (volts)	ΔE_p (volts)
1,2-DAAQ	+0.95	-	-
1,4-DAAQ	+0.77	+0.71	+0.06
1,5-DAAQ	+1.31	+0.85	+0.46

Isomer	$i_{p,c}$ (uA)	$i_{p,a}$ (uA)	$i_{p,c}/i_{p,a}$
1,2-DAAQ	0	116	-
1,4-DAAQ	34	50	0.68
1,5-DAAQ	15	28	0.54

Another factor[33] related to the conductivity of charge-transfer complex is electrochemical stability of its constituent radicals. TCNQ forms stable radical anions with appropriate donors and TTF forms stable radical cations with appropriate acceptors. These radical species stack face-to-face in the solid state and form one-dimensional conduction pathways. Other successful donor molecules, such as phenothiazine, perylene, p-phenylenediamine,[34] and ferrocene form stable free radicals via electrochemical oxidation in solution, as do TTF and TCNQ.

Electrochemical stability of an oxidized species can be measured as reversibility by cyclic voltammetry. The criteria are twofold: First, the potential difference ΔE_p between the forward (anodic) and reverse (cathodic) current waves at their maxima must be approximately 60 millivolts. This is derived from the relation

$$\Delta Ep = E_{p,a} - E_{p,c} = \frac{59.5 \text{ millivolts}}{n} \quad \text{at } 25°C^{35}$$

where n is the number of electrons involved in the oxidation. The second criterion is that the ratio of forward to reverse current, i(cathodic)/i(anodic), must be unity for a reversible process, indicating that the electrochemical intermediate is chemically stable and not subject to decomposition or reaction with another species.

Table 5 shows that only 1,4-DAAQ met the ΔE_p requirement. 1,5-DAAQ showed a reverse wave corresponding to the reduction of a decomposition product while 1,2-DAAQ did not show a reverse wave. The data did not show 1,4-DAAQ to be strictly reversible, however, with $i_{p,c}/i_{p,a}$ = 68% at 200 millivolts per second. Nonetheless, it did indicate that the

1,4-DAAQ radical cation had a measureable half-life, and does not rule out the possibility that it might be more stable in another solvent or in the solid state. While this evidence is not conclusive, it suggests a correlation between conductivity and electrochemical reversibility. It is felt that a more detailed cyclic voltammetric measurement could establish this point more firmly.

Electron Paramagnetic Resonance

Recent evidence has become available[36] which sheds light on the electronic structure of PH·I_2 (2:3), 1,4-DAAQ·I_2 (2:3), 1,4-DAAQ·$CuCl_2$ (1:1), and 1,4-DAAQ·$CuBr_2$ (3:2) in the solid state. Electron paramagnetic spectra were taken of these complexes at 298°K and 77°K on a Varian E-3 X-band Spectrometer, using quartz sample tubes and DPPH calibration. On the basis of observed g-factors, the absorptions shown in Figures 20 through 23 are consistent with the assignments given in Table 6. The free electron g-factor is 2.0023, and copper(II) of values typically lie between 2.1 and 2.4.[37] Halogen radicals in the solid state have not been observed.[38]

The data indicate that free-radical species are present in each complex along with copper(II) complexes where copper halides were involved. The free radical absorptions are assigned to the phenothiazinium radical cation in the PH·I_2 spectrum, and the radical cation of 1,4-DAAQ in 1,4-DAAQ-containing spectra. Their observation directly implies that partially complete charge transfer has occurred in each complex. These assignments are consistent with electrochemical studies in the literature[39] and

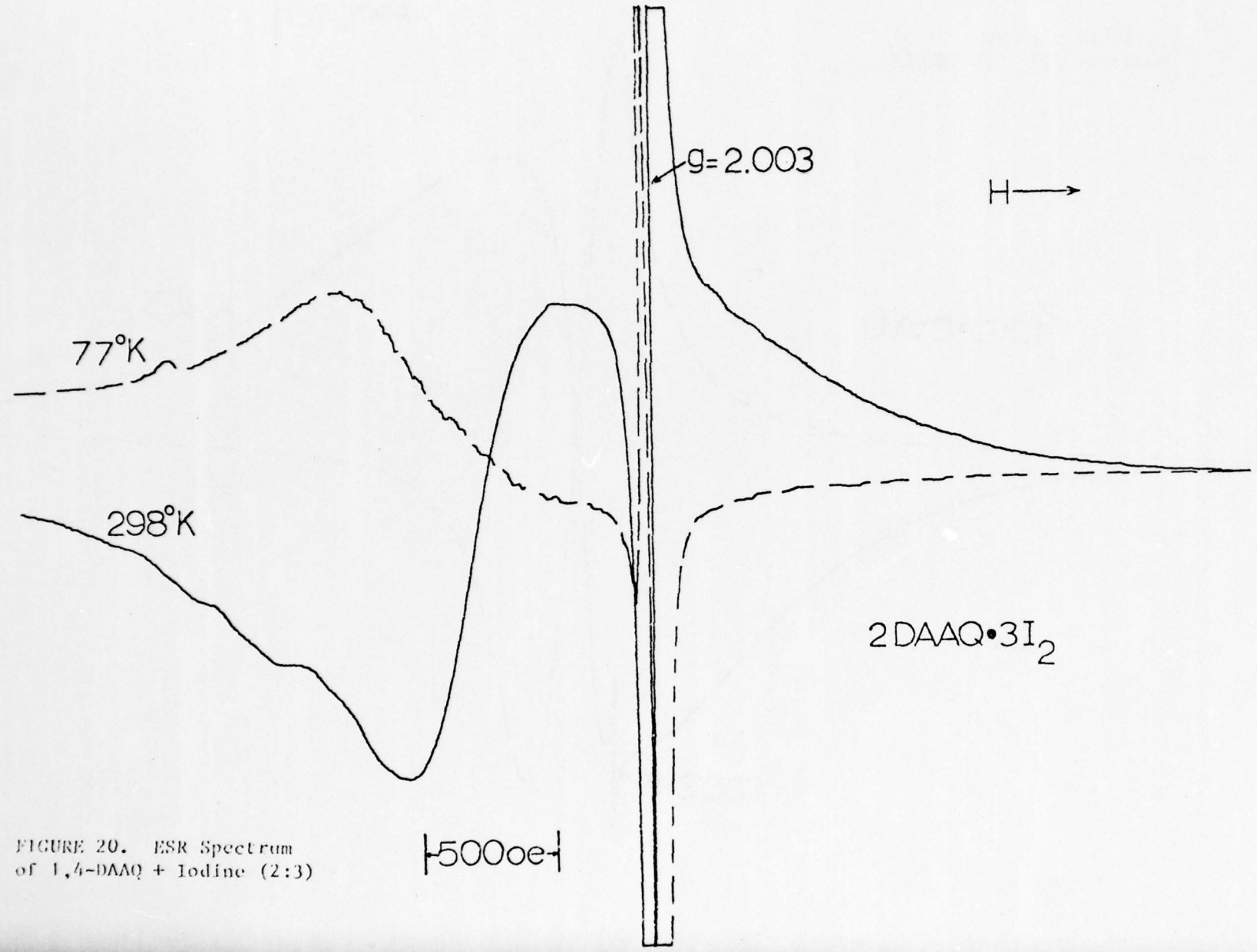

FIGURE 20. ESR Spectrum of 1,4-DAAQ + Iodine (2:3)

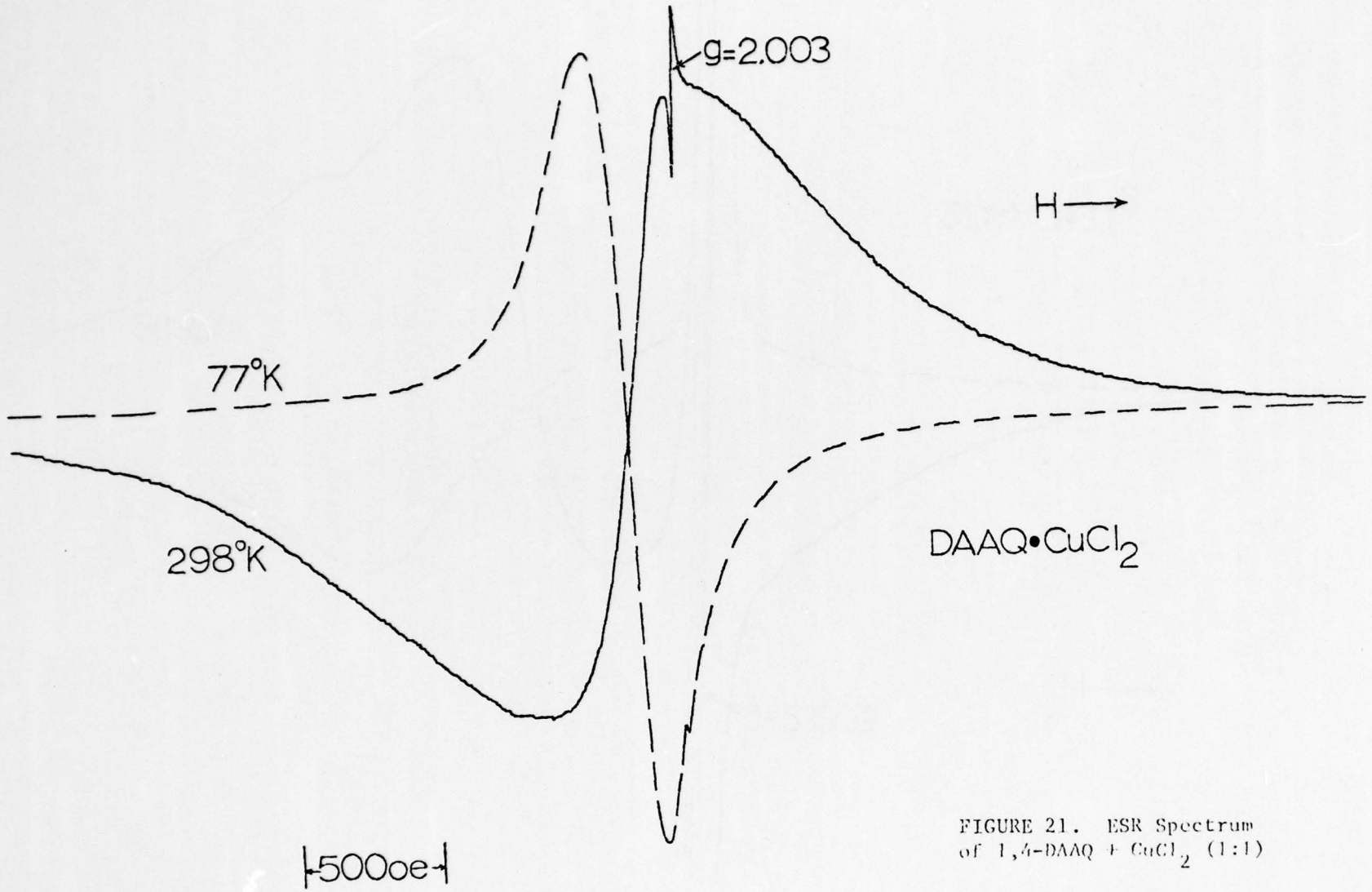

FIGURE 21. ESR Spectrum of 1,4-DAAQ + $CuCl_2$ (1:1)

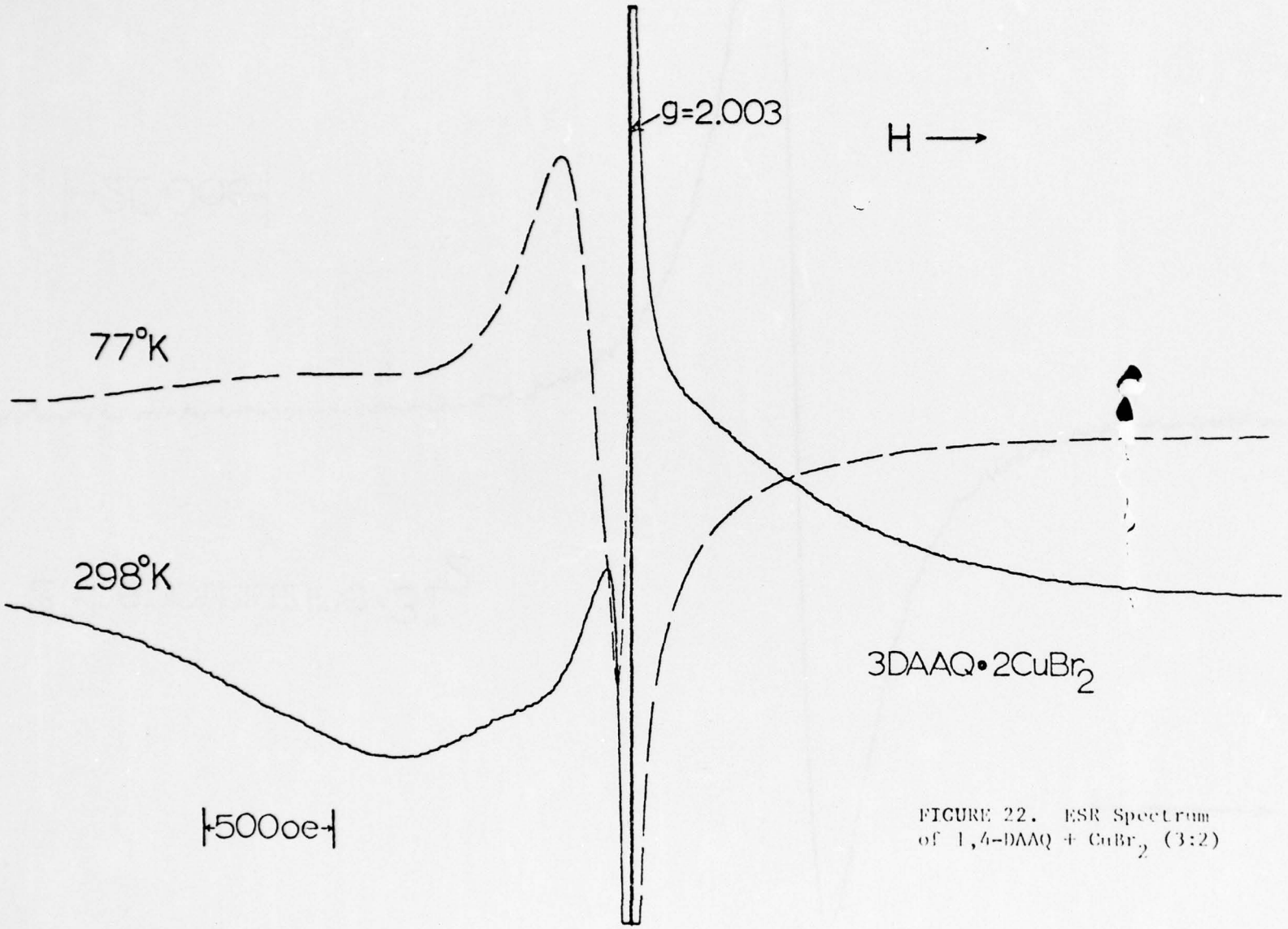

FIGURE 22. ESR Spectrum of 1,4-DAAQ + $CuBr_2$ (3:2)

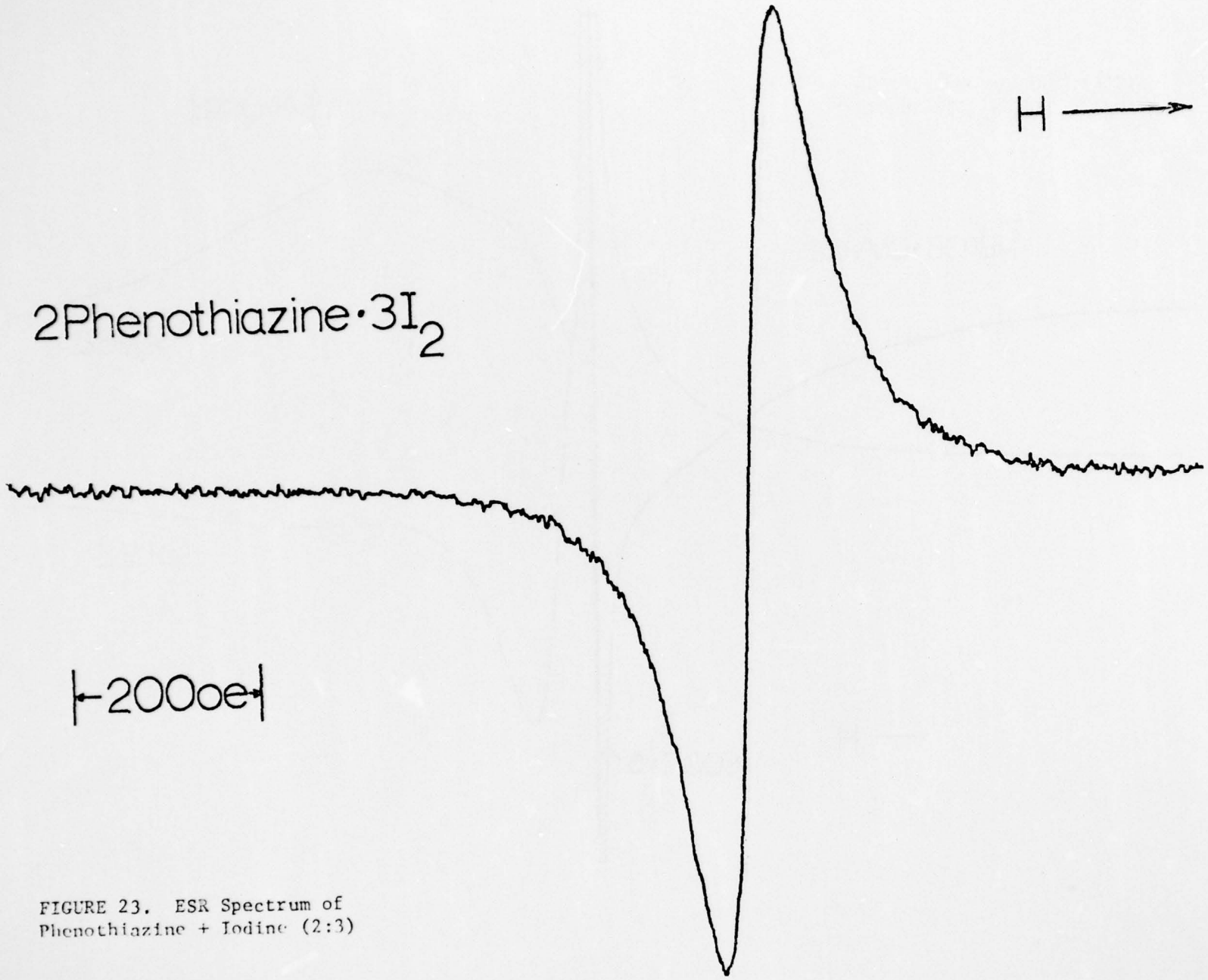

FIGURE 23. ESR Spectrum of Phenothiazine + Iodine (2:3)

TABLE 6

Electron Spin Resonance Band Assignments

Complex	g-factor	Assignment and Comment
phenothiazine·I_2 (2:3)	2.003	free radical, strong
1,4-DAAQ·I_2 (2:3)	2.003(77°K,298°K)	free radical, strong
	2.509(77°K)	unknown species
	2.571 (298°K)	unknown species
1,4-DAAQ·$CuCl_2$(1:1)	2.003 (77°K,298°K)	free radical, weak
	2.122 (77°K)	copper(II), dipolar-broadened
	2.118 (298°K)	copper(II), dipolar-broadened
1,4-DAAQ·$CuBr_2$(3:2)	2.003(77°K,298°K)	free radical, strong
	2.090 (77°K)	copper(II), dipolar-broadened
	2.085 (298°K)	copper(II), dipolar-broadened
	2.996 (77°K)	unknown species
	2.689 (298°K)	unknown species

the present work (see above) which suggest the existence of stable radical cations of phenothiazine and 1,4-DAAQ in acetonitrile. Abnormally high g-factors were also observed in two complexes, but the species giving rise to these absorptions are difficult to identify.

No hyperfine structure or zero-field splitting were observed for any complex, but the 1,4-DAAQ · I_2 spectrum showed a faint structure at approximately half the resonance field strength which may be a triplet state $\Delta Ms = \pm 2$ transition.[40] This is evidence of spin-spin coupling.[41] Interesting conclusions pertaining to the mechanism of conductivity in charge-transfer complexes have been drawn in the literature on the basis of spin-coupling evidence.[42]

Concluding Remarks

The results obtained here are consistent with the generalizations concerning the properties of donors essential for the formation of charge-transfer complexes: low oxidation potential, formation of stable radical cations, and planar structure. However, it would be simplistic to state that lowering the oxidation potential of the donor always causes a corresponding decrease in the resistivity of the charge-transfer salt, for this is not always observed in the literature. It may be concluded, therefore, that while the oxidation potential must be low for successful donors, it is not the sole factor contributing to the resistivity of the charge-transfer salt.

Furthermore, while the cyclic voltammetry evidence does not confirm that radical cations of 1,4-DAAQ are stable in acetonitrile for more than a short period of time, the electron spin resonance data almost surely

points to the existence of radical cations in the solid state. Cyclic voltammetry is regarded as a useful technique for the determination of radical stability, for it did definitely show that the radical cations of 1,2-DAAQ and 1,5-DAAQ are not stable and this observation conforms with the trend in resistivity given in Table 3. It is suggested that cyclic voltammetry be utilized more frequently in the study of the electronic properties of potential donors and acceptors.

The spring-loaded two-probe conductivity cell was shown to be efficient in screening the electrical properties of a large number of new compounds in compacted form. The use of three cells and a calibrated diode in the cryogenic apparatus was shown to be highly efficient in time expended and nitrogen coolant consumed.

It was noticed that contact resistance could be a problem and it is realized that this problem can be eliminated by using a four-probe electrode arrangement. Frequency-dependent measurements were found to be difficult due to the frequency restrictions inherent in the available electronic equipment and the conductivity cell. However, instruments that are loss-free over a wide range of frequency are available and the frequency response of the conductivity cell can be increased by reducing the amount of metal used in construction. Alternating-current bridge measurements or impedance measurements are considered to be feasible.

The charge-transfer salts formed by reaction of 1,4-DAAQ with molecular iodine and copper(II) halides were found to be semiconductors over the temperature range 77°K to room temperature. This room temperature resistivitives are on the order of 1×10^3 ohm-cm and their activation

energies were reported. The expotential activation law from band theory was not adhered to rigorously.

Likely structures for each of the 1,4-DAAQ adducts were suggested. The 1,4-DAAQ·I_2 salt is most likely to show a solid-state structure similar to that found in orthorhombic TTF·I_2,[43] namely, columns of TTF molecules stacked face-to-face contained in a matrix of polyiodide chains. It is also predicted that the 1,4-DAAQ·CuX_2 (X = Cl, Br) systems are coordination complexes, perhaps with stacked DAAQ molecules.

The PH·I_2 (2:3) charge-transfer salt has been reinvestigated with the following results: The room temperature resistivity determined in this work is higher than that reported in the literature, but the activation energy was found to be lower than that given in the literature by almost 50% (0.16 eV versus 0.088 eV). The electron spin resonance spectrum of this complex was consistent with the existence of phenothiazine radical cations in the solid state. Phenothiazine shows a stable radical cation in solution.[12]

To continue this study of 1,4-DAAQ charge-transfer salts it is important that single crystals be grown and the crystal structures be determined. To characterize the magnetic properties, magnetic susceptibility should be measured in the range 100° to 300°K. The susceptibility results should then be compared with the temperature-dependent conductivity.

To improve the technique of resistivity measurement, it is suggested that a new linear four-probe electrode system offered by Electro Scientific Industries, Inc.[44] be acquired. This system is small enough for single crystal work and utilizes spring-loaded electrodes for making electrical contact to uneven surfaces. The four-probe circuitry would provide contact-resistance-free measurement capability.

References

1. a) A.F. Garito and A.J. Heeger, Accounts of Chemical Research, 7, 232 (1974).
   b) R.C. Wheland and J.L. Gillson, J. Amer. Chem. Soc., 98, 3916 (1976).
   c) R.C. Wheland and A.J. Heeger, J. Amer. Chem. Soc., 98, 3926 (1976).
2. a) A.F. Garito and A.J. Heeger, Accounts of Chemical Research, 7, 232 (1974).
   b) R. Somoano, and V. Hadeck, S.P.S. Yen, A. Reinbaum, and R. Deck, J. Chem. Phys., 62, 1061 (1975).
3. L.S. Singer, J. Kommandeur, J. Chem. Phys., 34, 133 (1961).
4. A.F. Garito and A.J. Heeger, Accounts of Chem. Research, 7, 232 (1974).
5. D.S. Acker and W.R. Hertler, J. Amer. Chem. Soc., 84, 3370 (1962).
6. I.F. Shchegolev, Phys. Stat. Sol (a), 12, 9 (1972).
7. E.M. Engler, Chemical Technology, 6, 274 (1976).
8. a) Y. Matsunaga and Kosuke Shons, Bull. Chem. Soc. Japan, 43, 2007 (1970).
   b) F. Gutmann and H. Keyzer, J. Chem. Phys., 46, 1969 (1967).
9. P.F. Weller, (ed), Solid State Chemistry and Physics, Vol. 1 (Marcel Dekker, Inc., New York, N.Y.) 1973, p. 275.
10. a) L.R. Melby, R.J. Harder, W.R. Hertler, W. Mahler, R.E. Benson, and W.E. Mochel, J. Amer. Chem. Soc., 84, 3374 (1962).
    b) R.C. Wheland and J.L. Gillson, J. Amer. Chem. Soc., 98, 3916 (1976).
    c) J.G. Fitz, "Conductivity Measurements on Powdered and Polycrystalline Samples", Honors Thesis, Department of Chem., Univ. of North Carolina, 1975.

11. R.J. Lieb, "An Ionic Conductivity Study of Impurity-Vacancy Association in Silver Chloride and Silver Bromide," Ph.D. Thesis, Department of Physics and Astronomy,University ofNorth Carolina, Chapel Hill, 1976.

12. Private communication with Mr. David Hackleman, Department of Chemistry, UNC-CH.

13. J.G. Fitz, "Conductivity Measurements on Powdered and Polycrystalline Samples", Honors Thesis, Department of Chemistry, UNC-CH, 1975.

14. Lake Shore Cryotronics, Inc. publication entitled "Installation and Application Notes for Cryogenic Sensors".

15. C.M. Huggins, and A.H. Sharbaugh, J. Chem. Physics, 38, 393 (1963).

16. A.J. Senzel, (ed), Instrumentation in Analytic Chemistry, American Chemical Society, Washington, D.C., 1973, p. 249.

17. C.M. Huggins and A.H. Sharbaugh, J. Chem. Phys., 38, 393 (1963).

18. R.C. Wheland and J.L. Gillson, J. Amer. Chem. Soc., 98, 3916 (1976).

19. Kiethley Instruments publication, "Instruction Manual for Model 227 Current Source", p. 19.

20. F. Gutmann and H. Keyzer, J. Chem. Phys., 46, 1969 (1967).

21. R.J. Warmack, T.A. Callcott, and C.R. Watson, Phys, Rev., B, 12, 3336 (1975).

22. Walter Moore, Physical Chemistry (Prentice-Hall, Inc., Englewood Cliffs, New Jersey) Ch. 18, p. 877.

23. R.J. Warmack, T.A. Callott, and C.R. Watson, Phys. Rev., B, 12, 3336 (1975).

24. P.F. Weller, (ed), Solid State Chemistry and Physics, Vol. 1, (Marcel Dekker, Inc., New York, N.Y.) 1973, pp 199-200.

25. R.C. Weast, (ed), Handbook of Chemistry and Physics (The Chemical Rubber Company, Cleveland, Ohio), 1969, F-140.

26. E.M. Engler, Chemical Technology, 6, 274 (1976).

27. I.F. Shchegolev, Phys. Stat. Sol. (a), 12, 9 (1972).

28. P.R. Bevington, Data Reduction and Error Analysis for the Physical Sciences (McGraw-Hill Book Company) 1969, p. 119.

29. J.G. Fitz, "Conductivity Measurements on Powdered and Polycrystalline Samples", Honors Thesis, Department of Chemistry, UNC-CH, 1975.

30. E.S. Pysh and N.C. Yang, J. Amer. Chem. Soc., 85, 2124 (1963).

31. R.C. Wheland and J.L. Gillson, J. Amer. Chem. Soc., 98, 3916 (1976).

32. R.J. Warmack, T.A. Callcott, and C.R. Watson, Phys. Rev. B, 12, 3336 (1975).

33. A.F. Garito and A.J. Heeger, Accounts of Chemical Research, 7, 232 (1974).

34. L. Eberson and H. Schafer, Topics in Current Chemistry, Organic Electrochemistry (Springer-Verlag, New York) 1971, pp. 142-143.

35. Sawyer, D.T. and J.L. Roberts, Jr., Experimental Electrochemistry for Chemists (John Wiley and Sons, New York) 1974, p. 341.

36. J.R. Wasson and C.W. Andrews, unpublished results.

37. P.B. Ayscough, Electron Spin Resonance in Chemistry (Methuen and Co, Ltd., London) 1967, p. 47 and p. 188.

38. P.B. Ayscough, Electron Spin Resonance in Chemistry (Methuen and Co., Ltd., London) 1967, p. 335.

39. L. Eberson and H. Schaffer, Topics in Current Chemistry, Organic Electrochemistry (Springer-Verlag, New York) 1971, p. 143.

40. D.B. Chestnut and W.E. Phillips, J. Chem. Phys., 35, 1002 (1961).

41. This conclusion is supported by unpublished findings of J.R. Wasson.

42. a) L.S. Singer and J. Kommandeur, J. Chem. Phys., 34, 133 (1961).

b) D.B. Chestnut and P. Arthur, Jr., J. Chem. Phys., 36, 2969 (1962).

43. R.J. Warmack, T.A. Callcott, and C.R. Watson, Phys. Rev. B, 12, 3336 (1975).

44. I.E.E.E. Spectrum, November 1976, p. 71.

Acknowledgement

This research was supported by the Office of Naval Research.

TECHNICAL REPORT DISTRIBUTION LIST

	No. Copies
Office of Naval Research Arlington, Virginia 22217 Attn: Code 472	2
Office of Naval Research Arlington, Virginia 22217 Attn: Code 102IP	6
ONR Branch Office 536 S. Clark Street Chicago, Illinois 60605 Attn: Dr. George Sandoz	1
ONR Branch Office 715 Broadway New York, New York 10003 Attn: Scientific Dept.	1
ONR Branch Office 1030 East Green Street Pasadena, California 91106 Attn: Dr. R. J. Marcus	1
ONR Branch Office 760 Market Street, Rm. 447 San Francisco, California 94102 Attn: Dr. P. A. Miller	1
ONR Branch Office 495 Summer Street Boston, Massachusetts 02210 Attn: Dr. L. H. Peebles	1
Director, Naval Research Laboratory Washington, D.C. 20390 Attn: Library, Code 2029 (ONRL) Technical Info. Div. Code 6100, 6170	6 1 1
The Asst. Secretary of the Navy (R&D) Department of the Navy Room 4E736, Pentagon Washington, D.C. 20350	1
Commander, Naval Air Systems Command Department of the Navy Washington, D.C. 20360 Attn: Code 310C (H. Rosenwasser)	1

	No. Copie
Defense Documentation Center Building 5, Cameron Station Alexandria, Virginia 22314	12
U.S. Army Research Office P.O. Box 12211 Research Triangle Park, North Carolina 27709 Attn: CRD-AA-IP	
Commander Naval Undersea Research & Development Center San Diego, California 92132 Attn: Technical Library, Code 133	1
Naval Weapons Center China Lake, California 93555 Attn: Head, Chemistry Division	1
Naval Civil Engineering Laboratory Port Hueneme, California 93041 Attn: Mr. W. S. Haynes	1
Professor O. Heinz Department of Physics & Chemistry Naval Postgraduate School Monterey, California 93940	
Dr. A. L. Slafkosky Scientific Advisor Commandant of the Marine Corps (Code RD-1) Washington, D.C. 20380	1

TECHNICAL REPORT DISTRIBUTION LIST

	No. Copies
Dr. W. N. Lipscomb Department of Chemistry Harvard University Cambridge, Massachusetts 02138	1
Dr. R. M. Grimes Department of Chemistry University of Virginia Charlottesville, Virginia 22903	1
Dr. M. Tsutsui Department of Chemistry Texas A&M University College Station, Texas 77843	1
Dr. C. Quicksall Department of Chemistry Georgetown University 37th & O Streets Washington, D.C. 20007	1
Dr. M. F. Hawthorne Department of Chemistry University of California Los Angeles, California 90024	1
Dr. D. B. Brown Department of Chemistry University of Vermont Burlington, Vermont 05401	1
Dr. Alan Siedle National Bureau of Standards Department of Commerce Chemistry Section Washington, D.C. 20375	1
Dr. W. B. Fox Naval Research Laboratory Chemistry Division Code 5130 Washington, D.C. 20375	1
Dr. R. J. Lagow University of Texas Department of Chemistry Austin, Texas 78712	1
Dr. A. Cowley University of Texas Department of Chemistry Austin, Texas 78712	1
~~Dr. W. Hatfield~~ ~~University of North Carolina~~ ~~Department of Chemistry~~ ~~Chapel Hill, North Carolina 27514~~	1
Dr. D. Seyferth Massachusetts Institute of Technology Department of Chemistry Cambridge, Massachusetts 02139	1
Dr. M. H. Chisholm Princeton University Department of Chemistry Princeton, New Jersey 08540	1
Dr. B. Foxman Department of Chemistry Brandeis University Waltham, Massachusetts 02154	1